



Middle-Late Pleistocene Eastern Mediterranean nutricline depth and coccolith preservation linked to Monsoon activity and Atlantic Meridional Overturning Circulation

Alessandro Incarbona ^{a,*}, Gianluca Marino ^{b,c}, Enrico Di Stefano ^a, Michael Grelaud ^d, Nicola Pelosi ^e, Laura Rodríguez-Sanz ^{c,f}, Eelco J. Rohling ^{c,f}

^a Università degli Studi di Palermo, Dipartimento di Scienze della Terra e del Mare, Via Archirafi 22, 90134 Palermo, Italy

^b Centro de Investigación Mariña, Universidad de Vigo, GEOMA, Palaeoclimatology Lab, Vigo 36310, Spain

^c Research School of Earth Sciences, The Australian National University, Canberra, Australian Capital Territory 2601, Australia

^d Universitat Autònoma de Barcelona (UAB), Institute of Environmental Science and Technology (ICTA), Edifici Z, Carrer de les Columnes, Campus de la UAB, 08193 Bellaterra (Cerdanyola del Vallès), Barcelona, Spain

^e Consiglio Nazionale delle Ricerche, Istituto di Scienze del Patrimonio Culturale, Via Cardinale Guglielmo Sanfelice 8, 80134 Naples, Italy

^f Ocean and Earth Science, University of Southampton, Southampton SO14 3ZH, UK

ARTICLE INFO

Keywords:

Coccolith
F. profunda
 Holococcolith
 Eastern Mediterranean
 Middle Pleistocene
 Monsoon

ABSTRACT

The eastern Mediterranean Sea lies under the influence of high- and low-latitude climatic systems. The northern part of the basin is affected by Atlantic depressions and continental and polar air masses that promote intermediate and deep-water formation. The southern part is influenced by subtropical conditions and monsoon activity. Monsoon intensification results in enhanced freshwater discharge from the Nile River and other (now dry) systems along the North African margin. This freshwater influx into the Mediterranean Sea reduces surface water buoyancy loss. Disentangling the influences of these diverse climatic forcings is hindered by inherent proxy data limitations and by interactions between the climatic forcings. Here we use a wealth of published and new paleoclimate records across Termination II to understand the impacts of the higher latitude and subtropical/monsoon climate influences on coccolithophore ecology and holococcolith preservation in Aegean Sea sediment core LC21. We then use these findings to interpret coccolith assemblage variations at Ocean Drilling Program Site 967 (located nearby LC21, at the Eratosthenes Seamount) during multiple glacial-interglacial cycles across the Middle Pleistocene (marine isotopic stages 14–9). The LC21 analysis suggests that holococcolith preservation was enhanced during Heinrich Stadial 11 (~133 ka) and cold spell C26 (~119 ka). These two events have been previously linked to cold conditions in the North Atlantic and Atlantic Meridional Overturning Circulation weakening. We propose that associated atmospheric perturbations over the Mediterranean Sea promoted deep-water formation, and thus holococcolith preservation. Similarly, in the Middle Pleistocene (MIS 14–9) of Site 967, we observe temporal coincidence between ten episodes of enhanced holococcolith preservation and episodes of Atlantic Meridional Overturning Circulation slowdown. In Site 967, we also identified repeated fluctuations in placoliths and in *Florisphaera profunda*, which indicate nutricline depth variations. The development of a deep chlorophyll maximum is associated with the North Africa and wet phases, as recently observed using elemental proxy records at Site 967, during the deposition of sapropel layers. A further deep chlorophyll maximum development is identified during MISs 12 and 10, as a result of pycnocline and nutricline shoaling within the lower part of the photic zone due to glacial sea-level lowering and water mass transport reduction at both the Gibraltar and Sicily Straits. Finally, enhanced holococcolith preservation during cold/dry events is clearly correlated to weakened monsoon activity in both Africa and Asia.

* Corresponding author.

E-mail address: alessandro.incarbona@unipa.it (A. Incarbona).

1. Introduction

Paleoclimate reconstructions document the competing influence of southern versus northern climate systems on the hydrography and hydrology of the eastern Mediterranean Sea and its borderlands over a range of timescales (Emeis et al., 2000b; Grant et al., 2017, 2016; Lourens, 2004; Rohling et al., 2002b). During precession minima (Northern Hemisphere insolation maxima), the African monsoon intensified and shifted northward, with attendant enhancement of the freshwater release into the Mediterranean basin via large North African river systems and/or currently inactive wadis (Amies et al., 2019; Marino et al., 2009; Osborne et al., 2008; Rohling et al., 2002a; Rohling et al., 2015; van der Meer et al., 2007). This impacted the basin's hydrography and weakened or even shut down dense water formation, leading to oxygen starvation at depth and deposition of layers (sapropels) with elevated organic carbon concentrations (De Lange et al., 2008; Rohling et al., 2015; Rossignol-Strick et al., 1982). Millennial-scale climatic variations have been less well documented and appear to be associated with variations in the strength of the Atlantic Meridional Overturning Circulation (AMOC) (Grant et al., 2017, 2016; Stockhecke et al., 2016).

Coccolithophores are marine unicellular phytoplankton organisms living in the upper part of the water column. The ecology of coccolithophore species shows a strong sensitivity to modern gradients within the Mediterranean Sea and different species thrive in different areas, mainly in response to West-East temperature and nutrient gradients, water column dynamics, and meso-scale oceanographic features (Bonomo et al., 2012; D'Amario et al., 2017; Knappertsbusch, 1993; Oviedo et al., 2015). In the sedimentary archive, calcite coccolithophore remains (coccoliths) have been used successfully to infer orbital and suborbital variations in climate, productivity, and nutricline depth in oceans and marginal seas (Beaufort et al., 1997; Flores et al., 1997; Incarbone et al., 2013, 2010a; Marino et al., 2008; Molfino and McIntyre, 1990a; Rogalla and Andrleit, 2005). In the eastern Mediterranean Sea, coccolith-based paleoenvironmental reconstructions have been mostly aimed at assessing the shallow versus deep position of the nutricline within the photic layer and its relationship with the basin's freshwater budget, water mass circulation, and deep-sea ventilation during sapropel deposition (e.g., Grelaud et al., 2012). These studies attest to the development of a deep chlorophyll maximum (DCM) while organic carbon-rich layers were accumulating on the oxygen-starved eastern Mediterranean seafloor (Castradori, 1993; Giunta et al., 2003; Grelaud et al., 2012; Incarbone et al., 2019, 2011; Incarbone and Di Stefano, 2019; Maiorano et al., 2013; Negri et al., 1999; Principato et al., 2006; Triantaphyllou et al., 2009b, 2009a), corroborating findings based on other marine planktonic groups (Kemp et al., 1999; Meier et al., 2004; Rohling and Gieskes, 1989).

Here we present new data that complement a previous dataset of coccolith assemblages from south-eastern Aegean Sea core LC21 (Grelaud et al., 2012), across the penultimate glacial termination (termination II, T-II) and the last interglacial period, with a precise, radiometrically constrained chronology (Grant et al., 2012). This allows comparison of LC21 "coccolith proxies" with time series of palaeoclimate variability in the monsoon and the North Atlantic region (Cheng et al., 2009; Hodell et al., 2013), as well as atmospheric methane (CH_4) concentrations. Our combined dataset is probabilistically evaluated to decipher the amplitude and timing of change by quantitatively assessing the impact of chronological, analytical, and proxy uncertainties. We use this analysis as a proof of concept for new, highly resolved coccolith data from Ocean Drilling Program (ODP) Site 967 from the Eratosthenes Seamount, South of Cyprus, within the Nile Delta Basin province (Emeis et al., 1996). The new ODP 967 time series spans, at centennial-scale resolution, three glacial/interglacial cycles of the Middle Pleistocene, from glacial Marine Isotope Stage (MIS) 14 to interglacial MIS 9. Collectively, our new data and analyses provide insights into climate variability at orbital and sub-orbital timescales during both glacial and interglacial periods, complementing a wealth of

existing knowledge of the intervals of sapropel deposition. Specifically, we explore modifications in nutrient dynamics and holococcolith preservation during the Middle Pleistocene. These changes are compared with recently acquired variations in elemental abundances, elemental ratios, and climate indices for ODP Site 967 (Section 6.3) that portray the alternation of wet and dry North Africa periods at both orbital and sub-orbital timescales (Grant et al., 2017). Finally, we centre on the correlation between holococcolith preservation, AMOC, and boreal monsoon activity (both in Africa and in a wider Asian context) to assess: (i) the atmospheric impact of continental/polar air outbreaks on the eastern Mediterranean deep-sea ventilation and seafloor calcite preservation during cold stadials; and (ii) impact of millennial-scale atmospheric perturbations on the eastern Mediterranean Sea.

2. Environmental setting

A negative hydrological balance maintains a robust antiestuarine thermohaline circulation pattern in the Mediterranean Sea (Robinson and Golnaraghi, 1994). Surface Atlantic water (Modified Atlantic Water – MAW) enters the Mediterranean Sea and occupies the uppermost 100–200 m depth (Millot, 1999; POEM group, 1992). MAW spread out into the eastern Mediterranean Sea via the Mid-Mediterranean Jet and reaches the Eratosthenes Seamount where a quasi-permanent anticyclonic summer circulation exists, that is known as the Shikmona Gyre (Malanotte-Rizzoli et al., 2014; Pinardi and Masetti, 2000; POEM group, 1992). Levantine Intermediate Water (LIW) formation takes place close to the Eratosthenes Seamount (Ovchinnikov, 1984; POEM group, 1992). Eastern Mediterranean Deep Water (EMDW) forms in the Adriatic and Aegean Sea (Fig. 1) due to winter heat loss under the influence of intense Bora and Vardar winds (Malanotte-Rizzoli et al., 2014; POEM group, 1992).

Today, the eastern Mediterranean Sea is one of the most oligotrophic areas globally. Primary productivity is more than three times lower than in the western basin, in accordance with a similar nutrient depletion trend (Krom et al., 2010, 1991). Primary production is also seasonally controlled: higher productivity occurs in winter, after winter convection, while severe oligotrophy occurs in summer due to deepening of the thermocline and nutricline (Allen et al., 2002; Klein and Coste, 1984). The Eratosthenes region is classified as a no-bloom area by satellite-based chlorophyll analyses. The severe late spring-summer oligotrophy is followed by relatively higher chlorophyll values in winter (D'Ortenzio and Ribera d'Alcalà, 2009).

High- and low-latitude climate systems impact on the eastern Mediterranean Sea. In summer, subtropical high-pressure conditions cause stable dry and warm conditions throughout the Mediterranean area (Lionello, 2012). In winter, the North African subtropical high pressure is shifted southward, and cold and dry polar/continental air outbreaks occur into the eastern Mediterranean from the north (Lionello, 2012; Rohling et al., 2019, 2015). Expansion of the Siberian High is an important driver for advection of cold air toward the eastern Mediterranean. Intensification of the Siberian High during Holocene rapid climatic changes is thought to be an important driver of surface water cooling and atmospheric perturbations in the central-eastern Mediterranean Sea (Incarbone et al., 2008; Rohling et al., 2002b; Rohling et al., 2019). Prolonged and strengthened polar/continental air outbreaks promote sea surface heat loss and deep-water formation (Josey et al., 2011; Rohling et al., 2019; Velaoras et al., 2017).

3. Material and Methods

3.1. Sediment cores

ODP Site 967 (34°04.098'N, 32°43.523'E, 2553 m water depth) is located at the base of the northern slope of the Eratosthenes Seamount, a structure that emerges from the Nile Delta Cone (Fig. 1). Sediments are dominated by horizontal and sub-horizontal brown and light grey,

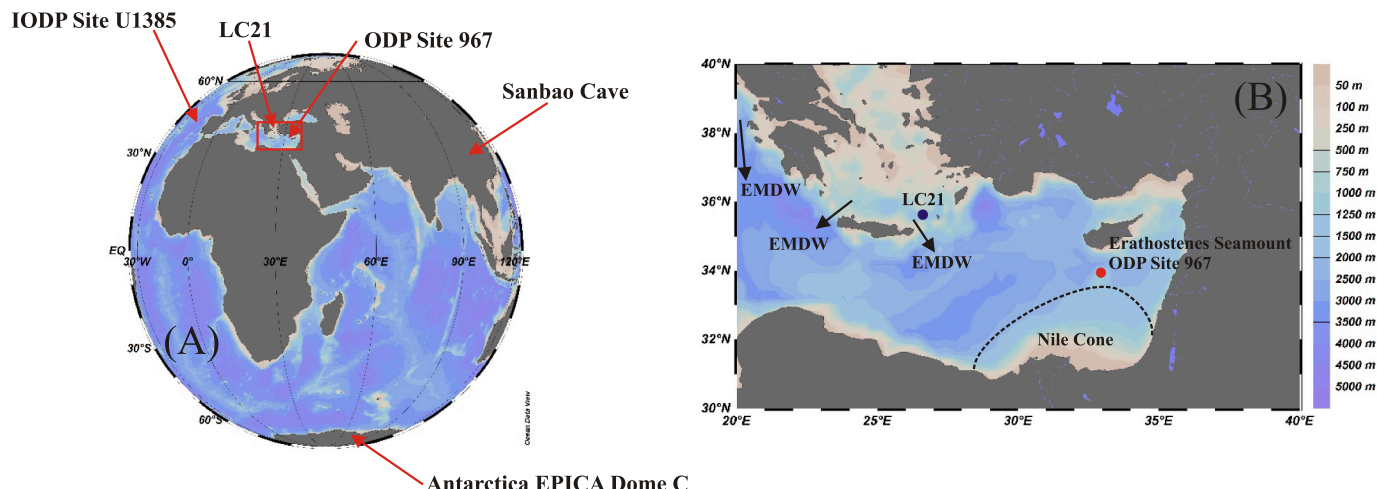


Fig. 1. location of ODP Site 967 and of records used for correlation. A) Red arrows indicate the location of International Ocean Discovery program (IODP) Site U1385 in the Iberian Margin, ODP Site 967 in the eastern Mediterranean, Core LC21 in the Aegean Sea, Sanbao Cave in China and EPICA Dome C in Antarctica. B) Inset map of the red box in A). The blue and red circles respectively indicate the location of core LC21 and ODP Site 967. The dashed line shows the Nile cone province. Black arrows point out the path of Eastern Mediterranean Deep-water from Adriatic and Aegean Sea. (For interpretation of the references to colour in this figure legend, the reader is referred to the web version of this article.)

bioturbated nannofossil ooze and nannofossil clay, intercalated with sapropels and turbidites (Emeis et al., 1996). Specifically, there are five sapropel layers that show signs of moderate bioturbation (S13, S12, S11, b and S10) in the studied interval (Emeis et al., 1996), while no turbidites and/or other sedimentary disturbances were identified (Konijnenhuijsen et al., 2014).

Sediment core LC21 (35°40'N, 26°35'E; 1522 m water depth) was recovered in 1995 by RV Marion Dufresne in the southeastern Aegean Sea (Fig. 1). Lithology consists of hemipelagic sediments, with visible sapropels (S1, S3, S4, and S5) and tephra layers (Grant et al., 2016; Satow et al., 2015).

3.2. Coccolith data

We carried out coccolith analyses at ODP Site 967 at 1 cm resolution between 14.80 and 21.49 m composite depth (mcd) (Emeis et al., 1996), for a total of 668 samples, which were analysed with a polarized microscope at $\sim 1000\times$ magnification. Rippled smear slides were prepared following standard procedures (Bown and Young, 1998). On average 350 specimens were identified following the taxonomic concepts for living coccolithophores of Young et al. (2003) and Jordan et al. (2004). Taxa were grouped as 'placoliths', 'miscellaneous group', 'upper photic zone (UPZ) group', 'lower photic zone (LPZ) group' and 'holococcoliths' (Di Stefano and Incarbone, 2004; Incarbone et al., 2010b). Placoliths include small placoliths, small *Gephyrocapsa*, *Gephyrocapsa muellerae*, and *Gephyrocapsa oceanica*. The miscellaneous group includes *Heliocosphaera* spp., *Coccolithus pelagicus*, *Syracosphaera hystrica*, *Pontosphaera* spp., *Calcidiscus leptoporus*, *Coronosphaera* spp., *Braarudosphaera* spp., *Oolithothus fragilis*, *Calciosolenia* spp., and specimens of all the other species. UPZ group includes *Syracosphaera pulchra*, *Umbellosphaera* spp., *Discosphaera tubifera*, *Rhabdosphaera* spp., *Umbilicosphaera* spp., and *Ceratolithus* spp.. LPZ group comprises *F. profunda*, which dominates the group, with negligible amounts of *Gladiolithus flabellatus* in a few samples. Holococcoliths include all the coccoliths produced during the haploid life-cycle stage (Incarbone et al., 2019).

The holococcolith analysis at Aegean Sea core LC21 was carried out by observation with a polarized microscope at about $1000\times$ magnification, following the standard procedure for rippled smear slides (Bown and Young, 1998). Holococcolith percentage values were evaluated on 102 samples versus heterococcoliths specimens, examining about 500 coccoliths. *Florisphaera profunda* percentage values at LC21 Aegean Sea

core were presented before (Grelaud et al., 2012), following the same procedure adopted in this study, and that earlier dataset is available at doi:<https://doi.org/10.1594/PANGAEA.805357>.

3.3. Statistical analysis of the time series

We use a Monte Carlo approach based on MATLAB coding (Marino et al., 2015; Thirumalai et al., 2016) to: (i) stack the $\delta^{18}\text{O}$ time series for different stalagmites (SB11, SB23, and SB25) from Sanbao Cave, China, that cover T-II and the last interglacial period (Cheng et al., 2009); (ii) calculate rates of $\delta^{18}\text{O}$ change in the Sanbao Cave stalagmites; (iii) probabilistically evaluate the chronological (Bazin et al., 2013; Veres et al., 2013) and measurement uncertainties associated with the time series of atmospheric methane (CH_4) concentrations from EPICA Dome C (EDC) (Loulergue et al., 2008); and (iv) probabilistically evaluate chronological and counting uncertainties associated with the *F. profunda* (Grelaud et al., 2012) and new holococcolith records for core LC21.

Speleothem $\delta^{18}\text{O}$ time series from Sanbao Cave have been probabilistically evaluated and stacked across the 140–110 ka interval. Input data for the Monte Carlo routine are sample ages with 1σ uncertainties, and speleothem $\delta^{18}\text{O}$ with 1σ uncertainties (Cheng et al., 2009). For each stalagmite (SB11, SB23, and SB25), individual data points are then separately and randomly sampled 10,000 times within their chronological and $\delta^{18}\text{O}$ uncertainties. The chronological uncertainties are evaluated using a random walk Monte Carlo routine that employs a Metropolis–Hastings approach to reject steps in the random walk that will result in age reversals (Rodríguez-Sanz et al., 2017). That is, we imposed a stratigraphic constraint (monotonic increase of age with depth, analogous to Rohling et al., 2014) to the data that are measured in a stratigraphically coherent manner along individual stalagmites. All realizations are then linearly interpolated on an equally spaced time scale and stacked to produce 10,000 speleothem $\delta^{18}\text{O}$ stacks with and without a correction that probabilistically quantifies the impacts of the global ^{18}O enrichment/depletion (Schrag et al., 2002) associated with ice-volume changes (Grant et al., 2012). Next, we calculated the 1st time derivative, to obtain rates of speleothem $\delta^{18}\text{O}$ change for each of the 10,000 ice-volume corrected 'stacks'. This is done by smoothing each realization using 0.75 kyr Gaussian window to remove sample-to-sample noise, which would result in spurious jumps in the estimated rates of change, and by then differentiating the smoothed realizations. Monte Carlo analysis of the EDC methane record and of the eastern

Mediterranean coccolith time series are performed using the same approach. Finally, the 10,000 iterations of each of these time series are linearly interpolated and the probability distribution assessed at each time step, thereby determining the 68% (16th–84th percentile) and 95% (2.5th–97.5th percentile) probability intervals and the probability maximum (PMAX, modal value) of the data.

4. Coccolith taxon ecology

Placoliths are so-called ‘r-strategist taxa’ that rapidly exploit nutrients in the photic zone (Baumann et al., 2005; Young, 1994). In the eastern Mediterranean Sea, placoliths bloom in winter, after nutrient fertilization (Di Stefano et al., 2011; Knappertsbusch, 1993; Triantaphyllou et al., 2004; Ziveri et al., 2000).

Florisphaera profunda is a deep photic zone species that indicates the occurrence of a deep nutricline (McIntyre and Molfino, 1996; Molfino and McIntyre, 1990a). In low- and middle-latitude open ocean regions, the relative abundance of this species is anticorrelated with primary productivity (Beaufort et al., 2001, 1997; Hernández-Almeida et al., 2019).

In the Mediterranean Sea, except for a limited area in the central part of the basin, there is no apparent relationship between *F. profunda* abundance and satellite-observed (surface) primary productivity levels (Hernández-Almeida et al., 2019; Incarbone et al., 2008). However, *F. profunda* has been generally used to decipher water column stratification and development of a deep nutricline due to monsoon-fuelled freshwater discharge in the eastern Mediterranean and entrainment of nutrients into the lower photic zone from below (Castradori, 1993; Grelaud et al., 2012; Incarbone et al., 2019; Negri et al., 1999; Triantaphyllou et al., 2009b). This occurs through the development of a distinct DCM in the eastern Mediterranean during sapropel deposition. DCM development resulted from nutrient entrainment into the photic zone from relatively buoyant intermediate waters that likely originated from the Adriatic Sea, while the volume of MAW inflow through the Sicily Strait was reduced (Myers et al., 1998; Rohling, 1991b; Rohling and Gieskes, 1989). Accordingly, relative abundances of placoliths and *F. profunda*, or their ratio, provide a robust indication of the depth of the nutricline in the eastern Mediterranean Sea. Specifically, presence (absence) of placoliths (*F. profunda*) in the coccolith assemblage reflects a shallow (deep) nutricline (Di Stefano et al., 2015; Flores et al., 2000; Molfino and McIntyre, 1990b).

The UPZ group consists of so-called ‘K-strategist taxa’, specialized to exploit a minimum uptake of nutrients in surface water (Bazzicalupo et al., 2020; Di Stefano and Incarbone, 2004; Young, 1994). Miscellaneous taxa reflect the lack of either an apparent distinctive ecological preference or of an understanding of their ecological preferences, with a potential weak K-strategy (Incarbone et al., 2010; Young, 1994). Holococcoliths prefer dwelling in warm, oligotrophic surface water and are abundant in the eastern Mediterranean Sea (D'Amario et al., 2017; Kleijne, 1991; Knappertsbusch, 1993; Dimiza et al., 2015; Oviedo et al., 2015; Skampa et al., 2019). Poor preservation of holococcoliths in sapropel S1 sediments was firstly recognised by Crudeli et al. (2006) and was later confirmed across the whole eastern Mediterranean, included the Eratosthenes Seamount (Incarbone et al., 2019; Incarbone and Di Stefano, 2019) and Pliocene sapropel layers in sedimentary sequences on Cyprus (Athanasios et al., 2015). Importantly, potential preservation of tiny holococcolith crystals improves when dense water renewal ensures vigorous ventilation/oxygenation of the seafloor, even during short reventilation episodes that “interrupt” sapropel deposition (Incarbone et al., 2019).

5. Chronology

The original shipboard age model by Sakamoto et al. (1998) at ODP Site 967 has since been revised, because of some inconsistent tuning to orbital insolation (Konijnendijk et al., 2014; Lourens et al., 2001). More

recently, Grant et al. (2017) developed a monsoon runoff (sapropel) proxy from the principal component analysis of sedimentary elemental data in ODP Site 967 that they tuned to precession minima. They use a zero phase lag, which relies upon the assumption that little or no lag exists when monsoon maxima did not immediately follow a high-amplitude glacial termination (Grant et al., 2016; Lourens et al., 2001). In this study, we adopt the chronology by Grant et al. (2017) for the coccolith data. Sedimentation rates between MIS 14 and MIS 9 range from 1.4 cm kyr⁻¹ to 3.9 cm kyr⁻¹, implying that the mean sampling resolution of our coccolith time series is about 340 years.

The LC21 chronology follows Grant et al. (2012) (see Section 6.1). The mean sedimentation rate is about 4.4 cm kyr⁻¹, with a mean sampling resolution of about 225 years.

6. Results and Discussion

6.1. Coccolith assemblages in Aegean Sea core LC21

Florisphaera profunda (Grelaud et al., 2012) and holococcoliths across T-II and the last interglacial in south-eastern Aegean core LC21 are used to evaluate their relationship with water column stratification and deep-sea ventilation, respectively. Several features make this core and the timespan that we target ideal to provide a ‘proof of concept’ for the interpretation of the new records from ODP Site 967 that spans multiple glacial-interglacial cycles. First, core LC21 has a radiometrically constrained chronology across T-II and the last interglacial period (Grant et al., 2012). This has been corroborated through comparison with western Mediterranean sediment cores and speleothem records, and it is consistent with the latest ice core chronology across the study interval (Marino et al., 2015). Second, prominent episodes of climate change punctuated T-II, including a multi-millennial Heinrich stadial associated with major freshwater discharge into the North Atlantic and AMOC slowdown (Deaney et al., 2017; Marino et al., 2015). Third, during the last interglacial period, an organic rich layer (sapropel S5) was deposited in the eastern Mediterranean under persistently anoxic or even euxinic conditions (Marino et al., 2007; Rohling et al., 2015, 2006). Sapropel S5 conditions developed in response to extensive monsoon-fuelled freshwater discharge along the North African Margin (Amies et al., 2019; Osborne et al., 2008; Rohling et al., 2002a; Rohling et al., 2004) that reduced surface salinity (van der Meer et al., 2007) and produced strong water column stratification (Amies et al., 2019; Grelaud et al., 2012; Marino et al., 2007; Rohling et al., 2006).

In Fig. 2a–c we show *F. profunda* relative abundances from core LC21 (Grelaud et al., 2012) with upper mixed layer depth fluctuations reconstructed for the same core (Amies et al., 2019), and with the contemporaneous EDC time series of atmospheric CH₄ concentrations and the Sanbao Cave δ¹⁸O stack, which are thought to reflect fluctuations in boreal monsoon intensity and attendant changes in the spatial coverage of tropical wetlands (Cheng et al., 2016, 2009, 2006; Möller et al., 2013; Petrenko et al., 2009). We present the *F. profunda* time series (Grelaud et al., 2012) on the radiometrically constrained chronology of Grant et al. (2012), as natural logarithm of the original data. Within uncertainties of the various records, we note a strong similarity between the LC21 *F. profunda* record and variations of both Sanbao Cave speleothem δ¹⁸O (Fig. 2a) and EDC CH₄ (Fig. 2b). Notably, a distinct *F. profunda* peak at ~129 ka appears contemporaneous with upper mixed layer thinning, with a maximum in the rates of Sanbao Cave δ¹⁸O change and with the CH₄ overshoot in EDC. This suggests: (i) synchronous intensification of the African and Asian monsoons at the onset of the last interglacial period, in line with what has been documented for the early Holocene (Fleitmann et al., 2003; Marino et al., 2009; Nicholson et al., 2020; Tierney et al., 2008); and (ii) a rapid increase in freshwater discharge into the eastern Mediterranean at the onset of the last interglacial monsoon maximum, quantified as up to ~8.8 times the modern pre-Aswan Nile discharge and responsible for the most intense thinning of the upper summer mixed layer (Amies et al., 2019).

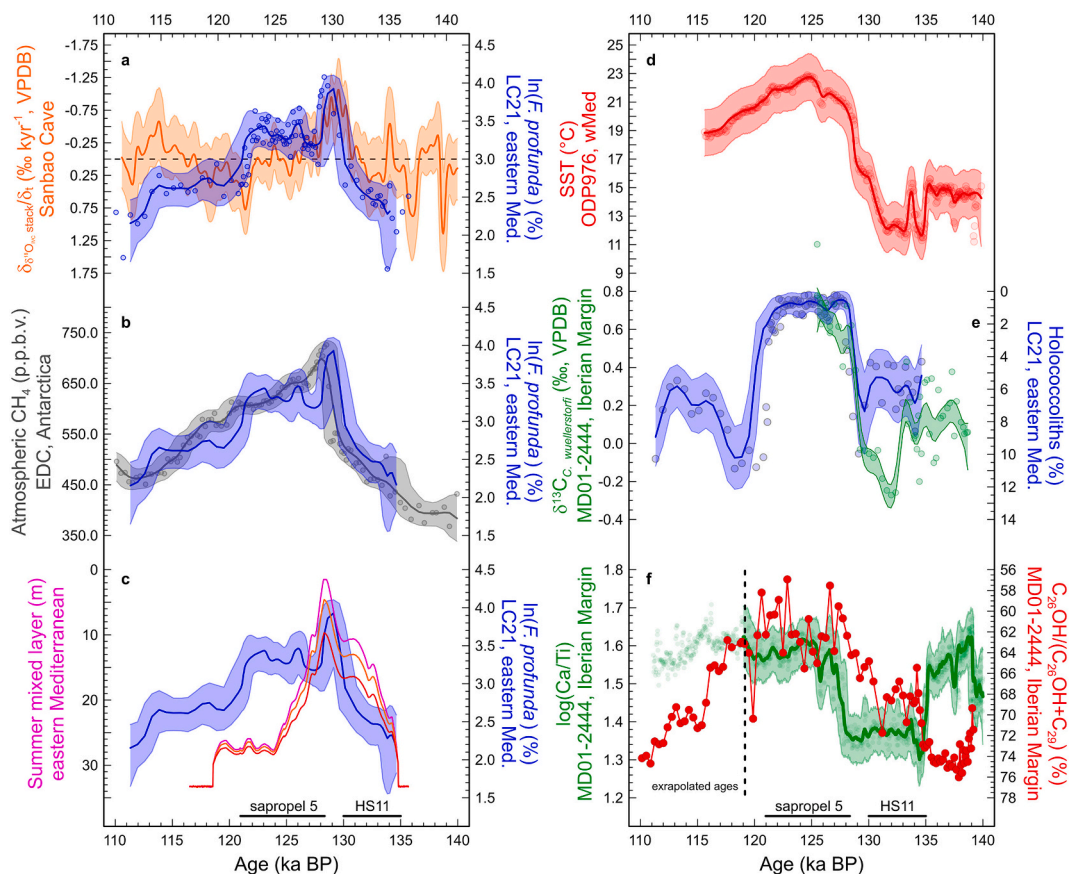


Fig. 2. plot of coccolith data in the Aegean Sea core LC21 and comparison with selected records. a) *Florisphaera profunda* percentage values (blue circles), expressed as natural logarithm (Grelaud et al., 2012). The 1st derivative of Sanbao Cave speleothem $\delta^{18}\text{O}$ (orange line) for each of the 10,000 ice-volume corrected ‘stacks’, following the chronology by Cheng et al. (2009) and after ice-volume correction. b) *Florisphaera profunda* percentage values (blue line), expressed as natural logarithm (Grelaud et al., 2012). Epica Dome C CH₄ (grey circles and grey line), following the Antarctic Ice Core chronology AICC2012 (Bazin et al., 2013) c) *Florisphaera profunda* percentage values (blue line), expressed as natural logarithm (Grelaud et al., 2012). Upper Summer Mixed Layer depth in the three different experiments by Amies et al. (2019) (respectively pink, orange and red lines for experiments A, B and C). d) Alkenone-derived SST (red circles) from the Alboran Sea (Martrat et al., 2014). e) Holococcoliths percentage values (blue circles, this study) and superimposed $\delta^{13}\text{C}$ values of the benthic foraminifera species *Cibicidoides wuellestorfi* from the Iberian Margin (green circles) (Martrat et al., 2007). f) Ca/Ti ratio, expressed as logarithm (green line), in sediments from the Iberian Margin (Hodell et al., 2015), superimposed to the C₂₆OH ratio from the same area (red circles) (Martrat et al., 2007). Thick lines represent the 3-pt running average and coloured shadows indicate the 95% confidence level. The sapropel S5 and HS11 extent is also shown. (For interpretation of the references to colour in this figure legend, the reader is referred to the web version of this article.)

Observation (ii) is particularly relevant because it alludes to the influence of the rates of monsoon intensification on stratification in the eastern Mediterranean. When large amounts of monsoon-fuelled freshwater are rapidly added to the basin, the strong evaporative climate of the Levant cannot keep up with sea-surface dilution (Rohling et al., 1991b) and the water column becomes strongly stratified (Rohling and Gieskes, 1989; Rohling et al., 2006; Marino et al., 2007; Athanasiou et al., 2015, 2017; Amies et al., 2019), causing shoaling of the pycnocline, the nutricline to be positioned at the base of the photic layer and the attendant development of a pronounced DCM.

In Fig. 2d–f, LC21 holococcolith data are compared with North Atlantic and western Mediterranean Sea records. It is evident that there is no or poor preservation of holococcoliths during sapropel S5 (Fig. 2e). Peaks of holococcoliths below S5 correlate with low alkenone-derived SSTs in the Alboran Sea (Martrat et al., 2014) (Fig. 2d) and with variations in AMOC strength proxies (Fig. 2e,f) from the Iberian Margin. Specifically, log (Ca/Ti), benthic foraminiferal $\delta^{13}\text{C}$, and C₂₆OH ratios (Hodell et al., 2015; Martrat et al., 2007) unequivocally indicate that AMOC had collapsed during Heinrich event HS11 (Böhm et al., 2015); we find that, at the same time, holococcolith preservation was enhanced. A similar relationship is evident above sapropel S5, especially with C₂₆OH ratio data (Fig. 2f), and may be correlated with North

Atlantic cold event C26 (Oppo et al., 2006, 2001; Tzedakis et al., 2018). Coupled ocean-atmosphere hindcasts suggest that the AMOC slowdown/shutdown may have propagated through the Mediterranean Sea in the form of major cooling and intense atmospheric perturbations (Manabe and Stouffer, 1997; Vellinga and Wood, 2002). Both cooling and atmospheric perturbations are major prerequisites for surface water buoyancy loss and deep-water formation, explaining enhanced Mediterranean bottom water ventilation during Heinrich and Stadial events in the last glacial, based on benthic foraminifera $\delta^{13}\text{C}$ and alcohol index records (Cacho et al., 2000; Sprovieri et al., 2012; Toucanne et al., 2012). Our new results from the Aegean Sea explicitly link holococcolith preservation to Heinrich and Stadial events in response to deep-water formation and seafloor ventilation increases in the Mediterranean Sea during those events.

6.2. Coccolith assemblages at ODP Site 967

At ODP Site 967, coccolith distribution patterns are compared (Fig. 3) with: (i) June 21st insulation at 65°N (Laskar et al., 2004); (ii) the benthic $\delta^{18}\text{O}$ composite record from ODP Sites 967 and 968 (Konijnendijk et al., 2015); and (iii) the LR04 benthic $\delta^{18}\text{O}$ stack (Lisicki and Raymo, 2005). Overall, coccolith assemblages are

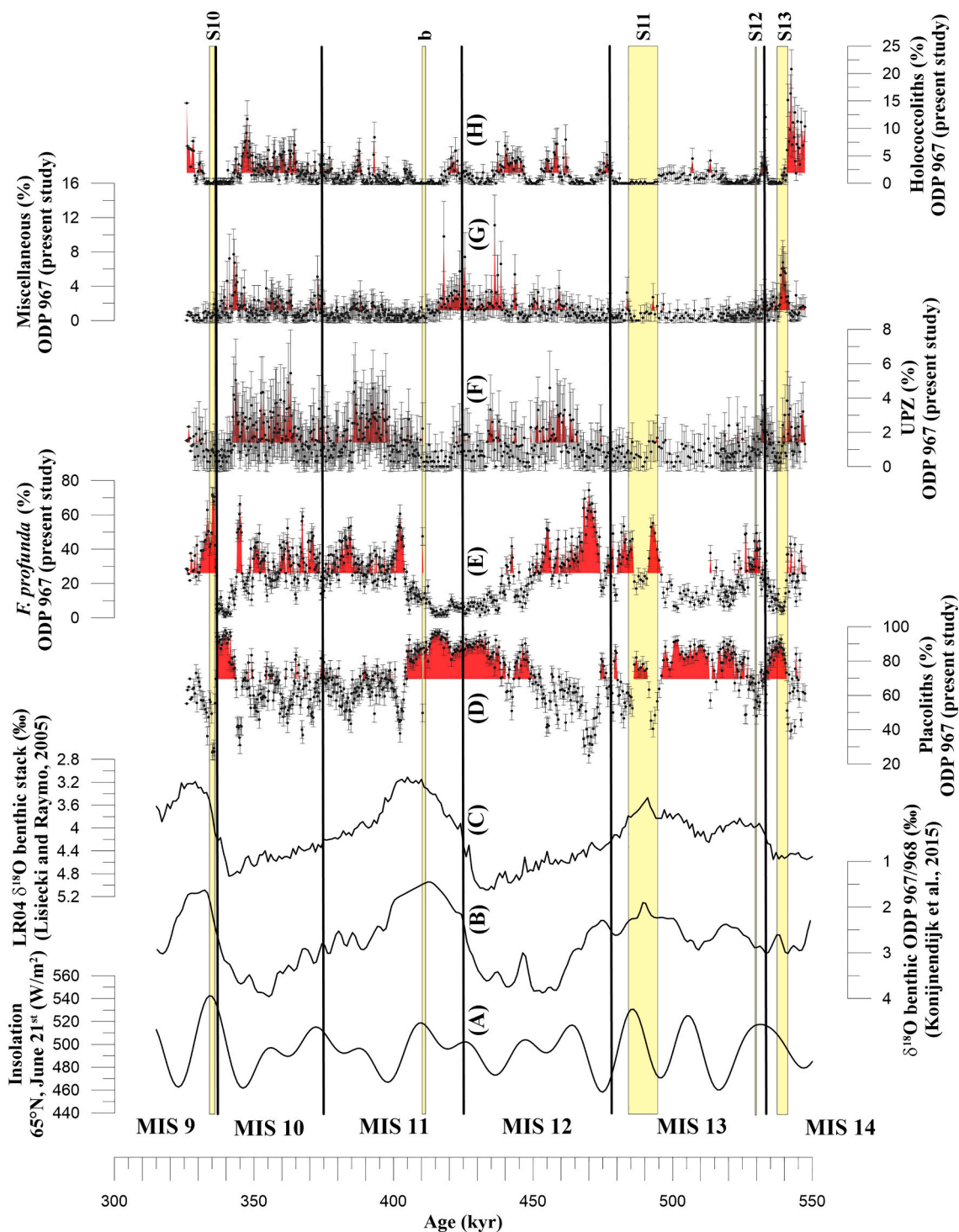


Fig. 3. plot of coccolith data at ODP Site 967 and comparison with selected records. A) June 21st insolation curve at 65°N (Laskar et al., 2004). B) Benthic $\delta^{18}\text{O}$ composite record from ODP Sites 967 and 968 (Konijnendijk et al., 2015). C) LR04 benthic $\delta^{18}\text{O}$ stack (Lisiecki and Raymo, 2005). D) Downcore percentage variations of Placoliths. E) Downcore percentage variations of *F. profunda*. F) Downcore percentage variations of UPZ taxa. G) Downcore percentage variations of Miscellaneous taxa. H) Downcore percentage variations of holococcoliths. Black horizontal bars show the error associated to countings for a 95% confidence level. Red filling indicates values higher than the total average percentage. Horizontal thick black lines indicate MIS boundaries from Lisiecki and Raymo (2005). Horizontal yellow boxes show visible sapropel layers in the ODP 967 composite section (Emeis et al., 2000a). (For interpretation of the references to colour in this figure legend, the reader is referred to the web version of this article.)

dominated by placoliths, with percentages between 25 and 98% (average = 70%, Fig. 3D). The deep photic zone species *F. profunda* features high-amplitude fluctuations between intervals in which it is barely occurring (1%) and intervals in which it becomes the dominant (up to 74%) (Fig. 3E). Placoliths' peak (low) abundances occur when

F. profunda percentages are at a minimum (maximum), as highlighted by the pronounced anticorrelation ($R^2 = 0.95, n = 668$) displayed in Fig. 4.

The observed alternating dominance of the placoliths and *F. profunda* (see above) at ODP Site 967 suggests that between MIS 14 and MIS 9 the upper water column in the easternmost Mediterranean Sea repeatedly

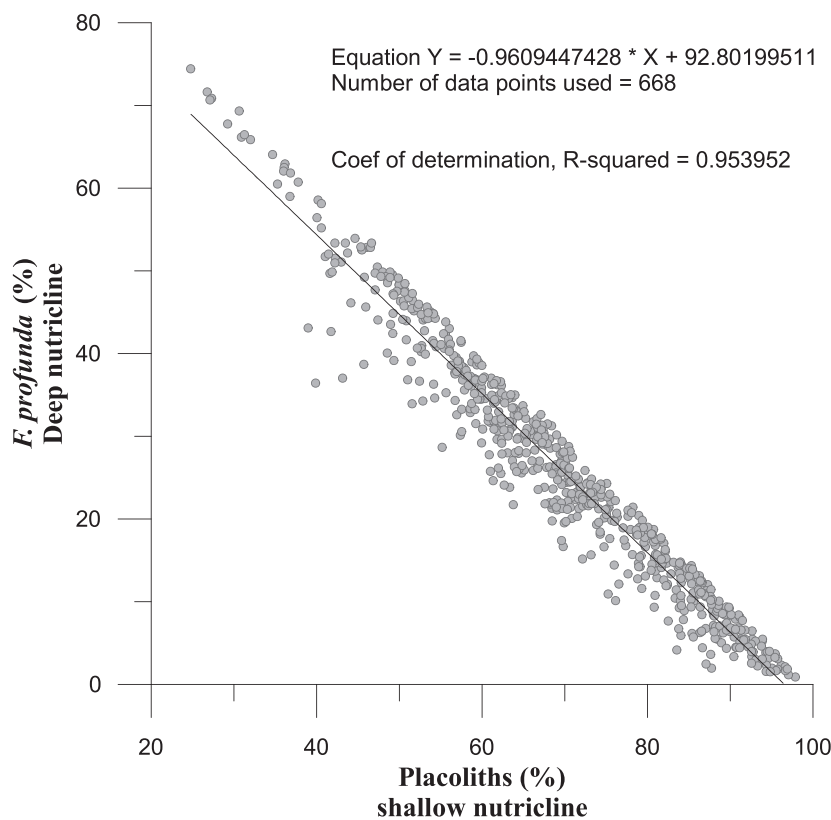


Fig. 4. scatter plot of placoliths and *F. profunda* percentage values at ODP Site 967. The black line shows the linear fit. The equation of the linear fit, R^2 correlation index and number of samples are also reported.

switched between dominant winter-induced fertilization (placoliths' peaks, shallow nutricline), similar to today's winter conditions (Knappertsbusch, 1993), and a predominantly DCM-focused productivity (*F. profunda*'s peaks, deep nutricline) during both glacial and interglacial periods. Shoaling of the pycnocline, which promoted a deep nutricline (DCM), in association with intensifications of the North African monsoon and sea-level lowering (Rohling and Gieskes, 1989; Rohling, 1991a, 1991b) is the most plausible explanation for the peak abundance of *F. profunda* at ODP Site 967 during sapropels and glacial periods, respectively. Accordingly, *F. profunda* would be particularly sensitive to nutrient (re)distribution within the photic zone, with intervals of positive shifts in the basins freshwater budget (monsoon maxima, Rohling, 1991b) and reduced water exchange at straits (glacial lowstands, Rohling, 1991a) both leading to enhanced stratification in the upper water column, shoaling of the pycnocline, and development of a nutricline at the base of the photic layer. This conceptual framework indicated by box-model calculations (Rohling, 1991a, 1991b) provides an explanation for the *F. profunda* peaks both in sapropel layers (e.g., S12, S11, b, S10) and during MIS 12 and MIS 10 glacial periods (see also Section 6.3).

The remaining three coccolith groups at Site 967 are largely subordinate. Low abundance of UPZ taxa (0.0–5.4%, 1.4% on average, Fig. 3F) and Miscellaneous taxa (0.0–11.1%, 1.2% on average, Fig. 3G) is unexpected in the severe oligotrophy of the eastern Mediterranean Sea, especially for UPZ taxa that include dominant coccolithophore species in summer/autumn (Knappertsbusch, 1993; Malinverno et al., 2009; Oviedo et al., 2015). However, living coccolithophore surveys show that winter production (placolith blooming) is about an order of magnitude higher than summer production, thereby explaining the apparent ecological contradiction in taxa proportions (Knappertsbusch, 1993).

Holococcolith percentage values range between 0.0 and 20.8%, 1.9% on average (Fig. 3H). As was the case in late Quaternary sapropels, tiny

holococcoliths are again not preserved in sapropel layers, but we also note that poor preservation extends far beyond sapropel layers.

6.3. Comparison between coccoliths, element ratios and climatic indices at ODP Site 967

Florisphaera profunda and holococcolith distribution patterns at ODP Site 967 (Fig. 5A–B) are compared with sedimentary elemental ratios and climatic indices from the same sedimentary sequence (Grant et al., 2017). A principal component analysis carried out on elemental proxies by these authors highlighted that principal components PC1 (not shown) and PC2 (Fig. 5D) account for 79% of variance and reflect terrigenous input and sapropel deposition (enhanced monsoon runoff), respectively. Moreover, aeolian dust fluxes (Fig. 5E) and a North Africa humidity/aridity index (Fig. 5F) were calculated and are also compared with coccolith abundance fluctuations.

Intensification of East African monsoon precipitation coincided with northward displacement of the Intertropical Convergence Zone (ITCZ) and subsequent intensification of precipitation over the catchment basins of the Nile and other rivers, which fuelled enhanced freshwater discharge along the wider North African margin into the eastern Mediterranean (Ehrmann et al., 2016; Rohling et al., 2002a; Rohling et al., 2015). *Florisphaera profunda* proliferates because it benefits from the nutricline positioned in deep photic zone and the establishment of a DCM (Castradori, 1993; Girone et al., 2013; Grelaud et al., 2012; Incarbone et al., 2011; Negri et al., 1999), following the rationale outlined above (Myers et al., 1998; Rohling, 1991a; Rohling and Gieskes, 1989). This scenario has been described for eastern Mediterranean sapropels and is further supported by the coupling of the *F. profunda* signal and enhanced humidity in North Africa that leads to enhanced monsoon runoff into the eastern Mediterranean, especially during S12, S11, b and S10 (Fig. 5). Also evident is decoupling between *F. profunda*

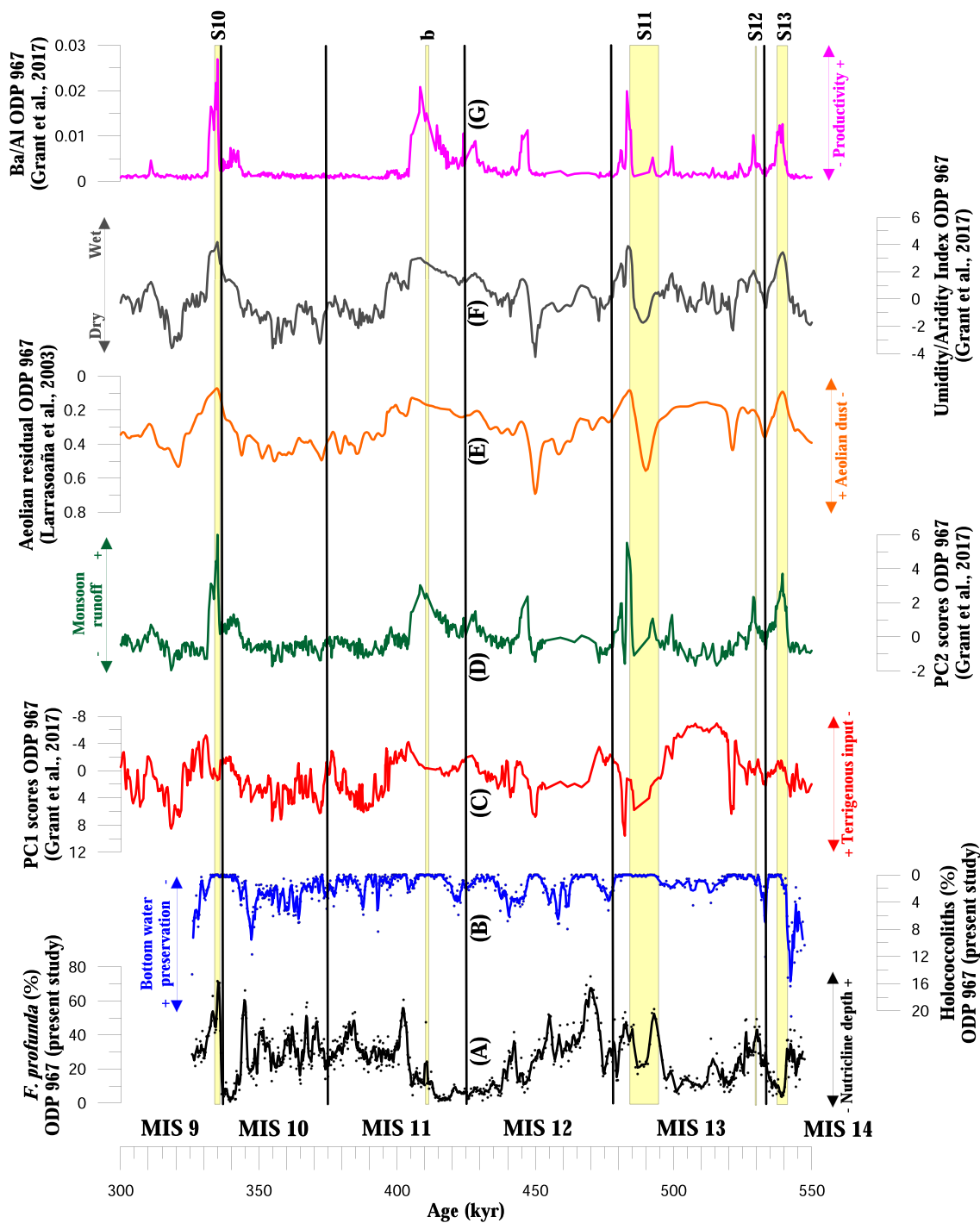


Fig. 5. coccolith, element ratios, indices and principal component scores at ODP Site 967. A) *Florisphaera profunda* percentage values (black circles, the black line is the 3-pt running average, this study). B) Holococcolith percentage values (blue circles, the blue line is the 3-pt running average, this study). C) Relative sea-level (Spratt and Lisicki, 2016). D) PC2 of elemental proxies that reflects sapropel/monsoon runoff layers (Grant et al., 2017). E) The Aeolian residual by Larrasoña et al. (2003) plotted by the Grant et al. (2017) chronology. F) The North Africa humidity/aridity index (Grant et al., 2017). G) The Ba/Al ratio (Grant et al., 2017). Horizontal thick black lines indicate MIS boundaries from Lisicki and Raymo (2005). Horizontal yellow boxes show visible sapropel layers in the ODP 967 composite section (Emeis et al., 2000a). (For interpretation of the references to colour in this figure legend, the reader is referred to the web version of this article.)

and the humidity/aridity index, for instance during glacial sapropel S13 and during sapropel layer b. This suggests that the climatic indices at ODP Site 967 reflect increased rainfall over North Africa and Sahara, without sufficient northward monsoon penetration that determines the intensity of monsoon-related runoff into the eastern Mediterranean Sea (Grant et al., 2017). Also, different nutrient dynamics may have developed during the glacial sapropel S13, with surface fertilization that

supports plankolith-bearing species competition.

However, the coccolith record at Site 967 suggests that *F. profunda* increases are a recurring feature of the record that is not necessarily associated with the deposition of organic-rich layers deposition on the eastern Mediterranean seafloor, especially in glacial episodes (Fig. 5A). The Ba/Al signal indicates that many sapropel layers have been partially oxidized (Fig. 5G), so that their currently visible extents do not represent

the original thickness of anoxic sediments. Yet, we argue that *F. profunda* peaks are not exclusively linked to the environmental changes associated with sapropel formation. Positive *Florisphaera profunda* peaks without a corresponding sapropel layer (be it visible, or oxidized) are evident in all eastern Mediterranean records that span sufficiently long time intervals (Castradori, 1993; Giunta et al., 2003; Maiorano et al., 2013; Negri et al., 1999; Triantaphyllou et al., 2010). The occurrence of *F. profunda* during glacial periods identifies a second mode of DCM development in the eastern Mediterranean, as proposed on the basis of planktonic foraminiferal assemblages (Rohling and Gieskes, 1989) and modeling (Myers et al., 1998; Rohling, 1991a). Again, the DCM development would be driven by the pycnocline and nutricline shoaling

within the lower part of the photic zone. But, for glaciials, the eustatic sea-level drop (Fig. 5C) would have been the main trigger mechanism, after reducing water mass transport at both Gibraltar and Sicily Straits and ultimately shoaling the pycnocline and nutricline depth up to ~80 m (Myers et al., 1998; Rohling, 1991a). However, the scattered *F. profunda* abundance signal in MISs 12 and 10 suggests that other factors may operate in conjunction with sea-level fall, for reducing water transport across the Gibraltar and Sicily Straits. Among these, less frequent and intense northern outbreaks in deep water production sites and the inflow of low-density meltwater from the Atlantic Ocean may have weakened the Mediterranean thermohaline circulation and may have caused transient reductions in the water transport at straits, like

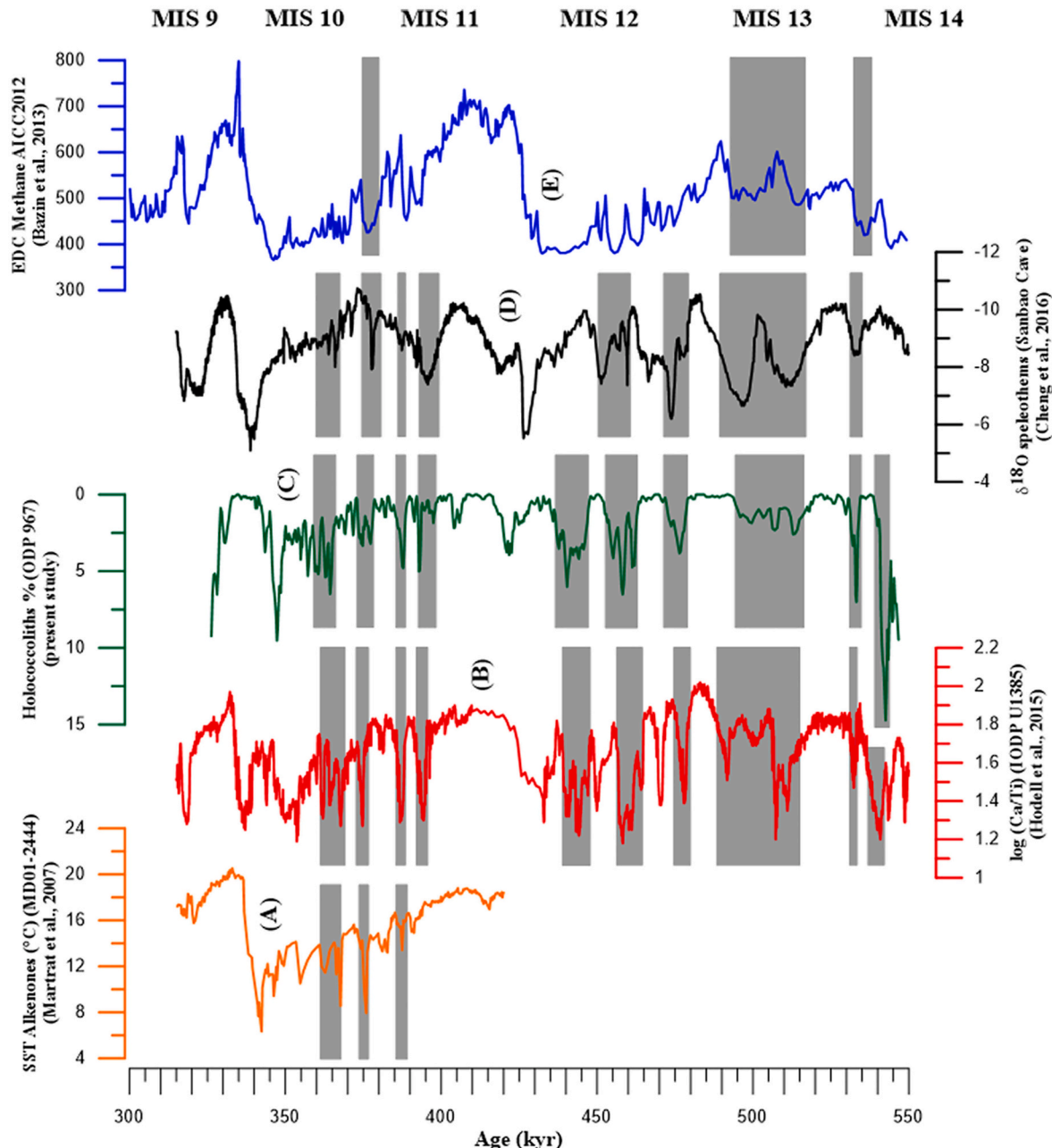


Fig. 6. correlation among Mediterranean, North Atlantic, Asian and Antarctica records. A) Alkenone-based SSTs ($^{\circ}\text{C}$) at Site MD01-2444, Iberian Margin (Martrat et al., 2007). B) Log (Ca/Ti) at IODP Site U1385, Iberian Margin (Hodell et al., 2015). Note the reversed axis. C) 3-pt running average of holococcolith percentage values at ODP Site 967, eastern Mediterranean Sea (present study). Note the reversed axis. D) $\delta^{18}\text{O}$ speleothem data at Sanbao Cave, China (Cheng et al., 2016). Note the reversed axis. E) Epica Dome C CH_4 , Antarctica (Bazin et al., 2013). Grey boxes indicate correlations: cooling and AMOC weakening/shutdown in the Iberian Margin (A, B), holococcolith preservation in the eastern Mediterranean seafloor (C), monsoon activity weakening in China (D) and EDC methane concentration decrease in Antarctica (see Section 6 for further explanation).

during last glacial cold spells (Sierro et al., 2005; Sprovieri et al., 2012; Toucanne et al., 2012; Azibeiro et al., 2021).

Holococcoliths are made of small calcite rhombohedra, arranged in different patterns. They are the most vulnerable coccoliths to selective dissolution (Roth and Coulbourn, 1982). Comparison between the new ODP 967 holococcolith record and the humidity/aridity index (Fig. 5B, F) shows strong similarities throughout the time span studied, which clearly point to the dissolution of haploid-life calcite remains at the Erathostenes seamount during humid phases. This agrees with the notion that surface buoyancy gain by freshwater river discharge negatively impacted deep-water formation in the eastern Mediterranean Sea, which enhanced organic carbon preservation (De Lange et al., 2008; Myers et al., 1998; Rohling et al., 2015) and, thus, worsened holococcolith preservation, like during sapropel S1 (Crudeli et al., 2006; Incarbone et al., 2019; Incarbone and Di Stefano, 2019) and sapropel S5 (Fig. 2, this study).

It is worth noting that the three major aeolian dust peaks during MIS 13–12 (Fig. 5E) did not match with increasing holococcolith preservation but fall within ‘no preservation’ intervals. Aeolian dust peaks are associated with weakened monsoon activity and North Africa dry periods, as seen from the Ti/Al ratio (Konijnendijk et al., 2015; Lourens et al., 2001; Wehausen and Brumsack, 2000; Ziegler et al., 2010), and would imply a lower freshwater input into the eastern Mediterranean Sea. Ideally, these conditions would enhance deep water formation, reduce organic matter preservation on the seafloor and increase preservation of holococcolith calcite. However, dust accumulation in marine cores depends on wind strength and direction (Moulin et al., 1997; Zabel et al., 1999). Thus, aeolian dust peaks are not necessarily tied to cooling and atmospheric perturbations that, for instance during the latest Quaternary, led to enhanced Mediterranean bottom water ventilation in coincidence of glacials and stadials (Cacho et al., 1999, 2000; Sprovieri et al., 2012; Toucanne et al., 2012).

6.4. AMOC slowdown, holococcolith preservation and monsoon weakening

In Fig. 6, North Atlantic geochemical records (Fig. 6A–B), Mediterranean holococcolith data (Fig. 6C), and oxygen isotopes of China speleothems (Fig. 6D) are plotted using their own original age models (Cheng et al., 2016; Grant et al., 2017; Hodell et al., 2015; Martrat et al., 2007). The grey boxes used for correlation are drawn and link correlative events in these various Northern Hemisphere records. Records shown in Fig. 6 help with outlining a concept of atmosphere/ocean interactions that resulted in the correlation between Northern Hemisphere climate variability and surface water ecosystem modifications and seafloor diagenesis in the eastern Mediterranean.

The correlation boxes in Fig. 6 are drawn assuming that AMOC slowdown/shutdown caused an atmospheric perturbation that impacted a vast area of the northern Hemisphere, including the eastern Mediterranean Sea, East African and Asian monsoon sites (Vellinga and Wood, 2002). The log (Ca/Ti) record from the Iberian Margin (Fig. 6B) is a proxy for millennial-scale variability (Hodell et al., 2015): minima indicate stadial/Heinrich phases during which the AMOC was severely weakened or collapsed (McManus et al., 2004, 1999). Previous studies based on $\delta^{13}\text{C}$, alcohol index and sortable silt records support the hypothesis that Mediterranean bottom water ventilation at least in the western sub-basin was more intense during glacial periods and stadial events (Cacho et al., 2000, 1999; Frigola et al., 2008; Sprovieri et al., 2012; Toucanne et al., 2012) and strengthened Mediterranean outflow into the Gulf of Cadiz and in the Iberian Margin (Sierro et al., 2020). Simultaneous enhancement of EMDW ventilation would have enhanced holococcolith preservation, as observed below and above sapropel S1 (Incarbone et al., 2019; Incarbone and Di Stefano, 2019) and during HS11 and C26 in the Aegean Sea (this study, Fig. 2). The physico-chemical processes in the seafloor microsystem by which tiny holococcolith calcite rhombohedra are preferentially preserved under oxic

conditions is not clear yet. Incarbone et al. (2019b) hypothesized a possible detrimental action of organic acid produced by bacteria under a dysoxic/anoxic state on the water/sediment interface, in analogy with results from modern surveys in the Gulf of California (Ziveri and Thunell, 2000). However, specific studies are needed to better understand the processes involved.

The link between AMOC slowdown/shutdown and East African, Indian, and Asian monsoon weakening is well-established (Deplazes et al., 2014; Porter and Zhisheng, 1995; Rohling et al., 2002; Rohling et al., 2006; Schulz et al., 1998; Sirocko et al., 1993; Tjallingii et al., 2008), and may involve severe drought development due to southward ITCZ displacement (Krebs and Timmermann, 2007; Vellinga and Wood, 2002; Zhang and Delworth, 2006). Yet, an ITCZ shift and associated Hadley cell changes likely explain only part of the impacts on monsoon circulation, which also depends on regional and local processes (Donohoe et al., 2013; Geen et al., 2020). For example, recent modeling shows that Northern Hemisphere glacial cooling, increased ice-sheet albedo, and sea-level lowering produce an anomalous thermal gradient between the Arabian Peninsula and the Arabian Sea that results in a weakened Walker circulation in the Indian Ocean and drought in the monsoon systems of the Indo-Pacific region (DiNezio et al., 2018). As mentioned before for the HS 11 and C26 cold spells (Section 6.1), AMOC slowdown/shutdown also produces cooling and intense atmospheric perturbations in the Mediterranean region (Manabe and Stouffer, 1997; Vellinga and Wood, 2002), facilitating deep-water formation and bottom water ventilation (Cacho et al., 2000; Sprovieri et al., 2012; Toucanne et al., 2012). Thus, AMOC slowdown/shutdown may have both strengthened cold and dry polar/continental air outbreaks and reduced Indian-African monsoon activity, with both processes conducive to enhanced EMDW production (the prerequisite for holococcolith preservation).

In Fig. 6, grey correlation boxes indicate a link between AMOC slowdown/shutdown phases (Fig. 6B) and both the heaviest oxygen isotopic values in Chinese Sanbao Cave speleothems (Fig. 6D) and enhanced holococcolith preservation in the Mediterranean (Fig. 6C).

The atmospheric CH₄ record from Antarctica ice cores (Fig. 6E) reflects emissions from boreal and monsoonal wetlands (Guo et al., 2012; Landais et al., 2010). The signal has been separated into three principal components, a glacial-interglacial forced component, a bi-hemispheric insolation driven component, and a millennial-scale oscillatory component, which respectively explain 80%, 15% and 5% of the variance (Guo et al., 2012). Glacial-interglacial cycles force globally synchronous monsoonal variations in methane emission. The other two forcings are hemispheric in nature, because of the two hemispheres’ anti-phasing for low-latitude summer insolation changes in ITCZ oscillations and for millennial-scale bipolar see-saw (strengthening/weakening) AMOC circulation (Guo et al., 2012). The limited number of grey correlation boxes between the Antarctic CH₄ signal and of Asian monsoon activity (Fig. 6D–E) suggests that the activity of Southern Hemisphere monsoon systems (South America, South Africa, Australia) have been a major driver of methane emission between 550 and 300 ka. However, we note the occurrence of three different peaks of Antarctic CH₄ during MIS 13, a signal which is also visible in Mediterranean holococcoliths and the China speleothem record (Fig. 6). This feature supports reduced emission from southern hemisphere methane sources during MIS 13 and an increased and synchronous emission from northern monsoons and boreal wetlands (Guo et al., 2012).

7. Conclusions

The chronology and age uncertainties of SE Aegean Sea core LC21 coccolith data, Iberian Margin geochemical records, $\delta^{18}\text{O}$ in the Sanbao Cave stalagmites, and atmospheric methane concentrations from EDC have been probabilistically assessed for the last interglacial and TII. The *F. profunda* peak at the base of sapropel S5 layer is contemporaneous with a maximum in the rates of $\delta^{18}\text{O}$ change in Sanbao Cave and with

the CH₄ overshoot in EDC, which suggests an African and Asian monsoon intensification at the onset of the last interglacial and the raising of the summer upper mixed layer depth. Holococcolith preservation was enhanced during Heinrich event HS11 and the C26 cold spell, when AMOC was severely weakened or collapsed. Cooling and atmospheric perturbations promoted surface-water buoyancy loss and deep-water formation, and thus increased Mediterranean bottom water ventilation rates. These results for LC21 explicitly link holococcolith preservation to episodes of enhanced deep-water formation and seafloor ventilation in the eastern Mediterranean Sea during Heinrich and Stadial events.

We also analysed 668 samples from ODP Site 967 to reconstruct variations in coccolithophore ecology in the region of the Eratosthenes Seamount (eastern Mediterranean Sea) between about 550 and 300 ka (Middle Pleistocene, MIS 14–9). Placoliths and *F. profunda* abundance fluctuations are strongly anticorrelated ($R^2 = 0.95$, $n = 668$) and together dominate the coccolith assemblages at Site 967, which suggests that the surface water environment repeatedly switched between predominant winter-induced fertilization (shallow nutricline) and predominant monsoon-induced deep nutricline conditions (and Deep Chlorophyll Maximum development) associated with a shoaling of the pycnocline to a position within the lower photic zone. In analogy with results for core LC21, Middle Pleistocene phases of enhanced monsoon runoff into the eastern Mediterranean appear to have caused shoaling of the pycnocline into the lower photic layer, which provides a deep nutricline that fosters *F. profunda* proliferation. A second mode of *F. profunda* proliferation and DCM development is seen in glacials, when the nutricline shoaled into the lower photic zone due to sea-level lowering that reduced water-mass transport through the main Mediterranean straits. Thus, our coccolithophore assemblage analyses corroborate earlier suggestions of such a phenomenon based on planktonic foraminiferal analyses (Rohling and Gieskes, 1989) and modeling (Myers et al., 1998; Rohling, 1991a).

Scattered but statistically significant peaks of holococcoliths (up to ~20%) mark increased carbonate preservation on the seafloor due to enhanced production of EMDW, which match changes in recently proposed North Africa aridity indices (Grant et al., 2017). Finally, holococcolith enhanced preservation during cold spells is linked to increased deep-water formation in the Mediterranean Sea, in response to Atlantic Meridional Overturning Circulation slowdown and weakened monsoon activity during Northern Hemisphere cold events.

Declaration of Competing Interest

The authors declare that they have no known competing financial interests or personal relationships that could have appeared to influence the work reported in this paper.

Data availability

Data will be made available on request.

Acknowledgments

We are grateful to an anonymous reviewer and to Fabienne Marret-Davies for their comments and suggestions. FFR2021 grant to A.I. is acknowledged. G.M. acknowledges support from the Universidade de Vigo's programme to attract excellent research talent (RR04092017), a Beatriz Galindo Fellowship (2020), and a generous start-up package. M.G. acknowledges support from the CALMED project (CTM2016-79547-R) and the Generalitat de Catalunya (MERS, 2014 SGR – 1356).

References

- Allen, J.I., Somerfield, P.J., Siddorn, J., 2002. Primary and bacterial production in the Mediterranean Sea: a modelling study. *J. Mar. Syst.* 33–34, 473–495. [https://doi.org/10.1016/S0924-7963\(02\)00072-6](https://doi.org/10.1016/S0924-7963(02)00072-6).
- Amies, J.D., Rohling, E.J., Grant, K.M., Rodríguez-Sanz, L., Marino, G., 2019. Quantification of African Monsoon Runoff during last interglacial Sapropel S5. *Paleoceanogr. Paleoclimatol.* 34, 1487–1516. <https://doi.org/10.1029/2019PA003652>.
- Athanasiou, M., Triantaphyllou, M.V., Dimiza, M.D., Gogou, A., Theodorou, G., 2015. Zanclean/Piacenzian transition on Cyprus (SE Mediterranean): calcareous nannofossil evidence of sapropel formation. *Geo-Mar. Lett.* 35, 367–385.
- Athanasiou, M., Boloubassi, I., Gogou, A., Klein, V., Dimiza, M.D., Parinos, C., Skampa, E., Triantaphyllou, M.V., 2017. Sea surface temperatures and environmental conditions during the 'warm Pliocene' interval (4.1–3.2 Ma) in the Eastern Mediterranean (Cyprus). *Glob. Planet. Chang.* 150, 46–57.
- Azibeiro, L.A., Siervo, F.J., Capotondi, L., Lirer, F., Andersen, N., González-Lanchas, A., Alonso-García, M., Flores, J.-A., Cortina, A., Grimalt, J.O., Martínez, B., Cacho, I., 2021. Meltwater flux from northern ice-sheets to the mediterranean during MIS 12. *Quat. Sci. Rev.* 268, 107108. <https://doi.org/10.1016/j.quascirev.2021.107108>.
- Baumann, K.-H., Andruleit, H., Böckel, B., Geisen, M., Kinkel, H., 2005. The significance of extant coccolithophores as indicators of ocean water masses, surface water temperature, and paleoproductivity: a review. *Palaontol. Z.* 79, 93–112. <https://doi.org/10.1007/bf03021756>.
- Bazin, L., Landais, A., Lemieux-Dudon, B., Toyé Mahamadou Kele, H., Veres, D., Parrenin, F., Martinerie, P., Ritz, C., Capron, E., Lipenkov, V., Loutre, M.-F., Raynaud, D., Vinther, B., Svensson, A., Rasmussen, S.O., Severi, M., Blunier, T., Leuenberger, M., Fischer, H., Masson-Delmotte, V., Chappellaz, J., Wolff, E., 2013. An optimized multi-proxy, multi-site Antarctic ice and gas orbital chronology (AICC2012): 120–800 ka. *Clim. Past* 9, 1715–1731. <https://doi.org/10.5194/cp-9-1715-2013>.
- Bazzicalupo, P., Maiorano, P., Girone, A., Marino, M., Combourieu-Nebout, N., Pelosi, N., Salgueiro, E., Incarbone, A., 2020. Holocene climate variability of the Western Mediterranean: surface water dynamics inferred from calcareous plankton assemblages. *The Holocene*. <https://doi.org/10.1177/0959683619895580>.
- Beaufort, L., Lancelot, Y., Camberlin, P., Cayre, O., Vincent, E., Bassinot, F., Labeyrie, L., 1997. Insolation cycles as a major control of equatorial Indian Ocean primary production. *Science* 278, 1451–1454.
- Beaufort, L., de Garidel-Thoron, T., Mix, A.C., Pisias, N.G., 2001. ENSO-like forcing on oceanic primary production during the late Pleistocene. *Science* 293, 2440–2444. <https://doi.org/10.1126/science.293.5539.2440>.
- Böhm, E., Lippold, J., Gutjahr, M., Frank, M., Blaser, P., Antz, B., Fohlmeister, J., Frank, N., Andersen, M.B., Deininger, M., 2015. Strong and deep Atlantic meridional overturning circulation during the last glacial cycle. *Nature* 517, 73–76. <https://doi.org/10.1038/nature14059>.
- Bonomo, S., Grelaud, M., Incarbone, A., Malinverno, E., Placenti, F., Bonanno, A., Stefano, E.D., Patti, B., Sprovieri, M., Genovese, S., Rumolo, P., Mazzola, S., Zgozi, S., Ziveri, P., 2012. Living Coccolithophores from the Gulf of Sirte (Southern Mediterranean Sea) during the summer of 2008. *Micropaleontology* 58, 487–503.
- Bown, Paul R., Young, J.R., 1998. Techniques. In: Bown, P.R. (Ed.), *Calcareous Nannofossil Biostratigraphy*. Chapman and Kluwer Academic, London, pp. 16–28.
- Cacho, I., Grimalt, J.O., Pelejero, C., Canals, M., Siervo, F.J., Flores, J.A., Shackleton, N., 1999. Dansgaard-Oeschger and Heinrich event imprints in Alboran Sea paleotemperatures. *Paleoceanography* 14, 698–705. <https://doi.org/10.1029/1999PA900044>.
- Cacho, I., Grimalt, J.O., Siervo, F.J., Shackleton, N., Canals, M., 2000. Evidence for enhanced Mediterranean thermohaline circulation during rapid climatic coolings. *Earth Planet. Sci. Lett.* 183, 417–429. [https://doi.org/10.1016/S0012-821X\(00\)00296-X](https://doi.org/10.1016/S0012-821X(00)00296-X).
- Castradori, D., 1993. Calcareous nannofossils and the origin of Eastern Mediterranean sapropel. *Paleoceanography* 8, 459–471.
- Cheng, H., Edwards, R.L., Wang, Y., Kong, X., Ming, Y., Kelly, M.J., Wang, X., Gallup, C.D., Liu, W., 2006. A penultimate glacial monsoon record from Hulu Cave and two-phase glacial terminations. *Geology* 34, 217–220. <https://doi.org/10.1130/G22289.1>.
- Cheng, H., Edwards, R.L., Broecker, W.S., Denton, G.H., Kong, X., Wang, Y., Zhang, R., Wang, X., 2009. Ice age terminations. *Science* (80–) 326, 248–252. <https://doi.org/10.1126/science.1177840>.
- Cheng, H., Edwards, R.L., Sinha, A., Spötl, C., Yi, L., Chen, S., Kelly, M., Kathayat, G., Wang, X., Li, X., Kong, X., Wang, Y., Ning, Y., Zhang, H., 2016. The Asian monsoon over the past 640,000 years and ice age terminations. *Nature* 534, 640–646. <https://doi.org/10.1038/nature18591>.
- Crudeli, D., Young, J.R., Erba, E., Geisen, M., Ziveri, P., de Lange, G.J., Slomp, C.P., 2006. Fossil record of holococcoliths and selected hetero-holococcolith associations from the Mediterranean (Holocene-late Pleistocene): evaluation of carbonate diagenesis and palaeoecological-palaeocenographic implications. *Palaeogeogr. Palaeoclimatol. Palaeoecol.* 237, 191–212. <https://doi.org/10.1016/j.palaeo.2005.11.022>.
- D'Amario, B., Ziveri, P., Grelaud, M., Oviedo, A., Kralj, M., 2017. Coccolithophore haploid and diploid distribution patterns in the Mediterranean Sea: can a haplo-diploid life cycle be advantageous under climate change? *J. Plankton Res.* 39, 781–794. <https://doi.org/10.1093/plankt/fbx044>.
- De Lange, G.J., Thomson, J., Reitz, A., Slomp, C.P., Principato, M.S., Erba, E., Corselli, C., 2008. Synchronous basin-wide formation and redox-controlled preservation of a Mediterranean sapropel. *Nat. Geosci.* 1, 606–610. <https://doi.org/10.1038/ngeos283>.

- Deaney, E.L., Barker, S., van de Flierdt, T., 2017. Timing and nature of AMOC recovery across Termination 2 and magnitude of deglacial CO₂ change. *Nat. Commun.* 8, 14595. <https://doi.org/10.1038/ncomms14595>.
- Deplazes, G., Lückge, A., Stuut, J.-B.W., Pätzold, J., Kuhlmann, H., Husson, D., Fant, M., Haug, G.H., 2014. Weakening and strengthening of the Indian monsoon during Heinrich events and Dansgaard-Oeschger oscillations. *Paleoceanography* 29, 99–114. <https://doi.org/10.1002/2013PA002509>.
- Di Stefano, A., Foresi, L.M., Incarbone, A., Sprovieri, M., Vallefuoco, M., Iorio, M., Pelosi, N., Di Stefano, E., Sangiorgi, P., Budillon, F., 2015. Mediterranean coccolith ecobiostratigraphy since the penultimate Glacial (the last 145,000 years) and ecobioevent traceability. *Mar. Micropaleontol.* 115 <https://doi.org/10.1016/j.marmicro.2014.12.002>.
- Di Stefano, E., Incarbone, A., 2004. High-resolution palaeoenvironmental reconstruction of ODP Hole 963D (Sicily Channel) during the last deglaciation based on calcareous nannofossils. *Mar. Micropaleontol.* 52 <https://doi.org/10.1016/j.marmicro.2004.04.009>.
- Di Stefano, E., Incarbone, A., Bonomo, S., Pelosi, N., 2011. Coccolithophores in Water Samples and Fossil Assemblages in Sedimentary Archives of the Mediterranean Sea: A Review. *New Oceanography Research Developments: Marine Chemistry, Ocean Floor Analyses and Marine Phytoplankton*.
- Dimiza, M.D., Triantaphyllou, M.V., Malinverno, E., Psarra, S., Karatsolis, B., Mara, P., Lagaria, A., Gogou, A., 2015. The composition and distribution of living coccolithophores in the Aegean Sea (NE Mediterranean). *Micropaleontology* 61, 521–540.
- DiNezio, P.N., Tierney, J.E., Otto-Bliesner, B.L., Timmermann, A., Bhattacharya, T., Rosenbloom, N., Brady, E., 2018. Glacial changes in tropical climate amplified by the Indian Ocean. *Sci. Adv.* 4, eaat9658. <https://doi.org/10.1126/sciadv.aat9658>.
- Donohoe, A., Marshall, J., Ferreira, D., Mcgee, D., 2013. The relationship between ITCZ location and cross-equatorial atmospheric heat transport: from the seasonal cycle to the last glacial maximum. *J. Clim.* 26, 3597–3618. <https://doi.org/10.1175/JCLI-D-12-00467.1>.
- D'Ortenzio, F., Ribera d'Alcalà, M., 2009. On the trophic regimes of the Mediterranean Sea: a satellite analysis. *Biogeosciences* 6, 139–148. <https://doi.org/10.5194/bg-6-139-2009>.
- Ehrmann, W., Schmiedl, G., Seidel, M., Krüger, S., Schulz, H., 2016. A distal 140,000-year sediment record of Nile discharge\backslashnewline and East African monsoon variability. *Clim. Past* 12, 713–727. <https://doi.org/10.5194/cp-12-713-2016>.
- Emeis, K.C., Sakamoto, T., Wehausen, R., Brumsack, H.J., 2000a. The sapropel record of the eastern Mediterranean Sea - results of Ocean Drilling Program Leg 160. *Palaeogeogr. Palaeoclimatol. Palaeoecol.* 158, 371–395. [https://doi.org/10.1016/S0031-0182\(00\)0059-6](https://doi.org/10.1016/S0031-0182(00)0059-6).
- Emeis, K.C., Struck, U., Schulz, H.M., Rosenberg, R., Bernasconi, S., Erlenkeuser, H., Sakamoto, T., Martinez-Ruiz, F., 2000b. Temperature and salinity variations of Mediterranean Sea surface waters over the last 16,000 years from records of planktonic stable oxygen isotopes and alkenone unsaturation ratios. *Palaeogeogr. Palaeoclimatol. Palaeoecol.* 158, 259–280. [https://doi.org/10.1016/S0031-0182\(00\)0053-5](https://doi.org/10.1016/S0031-0182(00)0053-5).
- Emeis, K.-C., Robertson, A.H.F., Richter, C., Party, S., Emeis, K.-C., Robertson, A.H.F., Richter, C., 1996. Site 967. In: *Proceedings of the Ocean Drilling Program, Initial Reports, Leg 160*, pp. 215–287.
- Fleitmann, D., Burns, S.J., Mudelsee, M., Neff, U., Kramers, J., Mangini, A., Matter, A., 2003. Holocene forcing of the Indian Monsoon Recorded in a Stalagmite from Southern Oman. *Science* (80-.300), 1737–1739. <https://doi.org/10.1126/science.1083130>.
- Flores, J.A., Siervo, F.J., Francés, G., Vazquez, A., Zamarreno, I., 1997. The last 100,000 years in the western Mediterranean: sea surface water and frontal dynamics as revealed by coccolithophores. *Mar. Micropaleontol.* 29, 351–366.
- Flores, J.A., Bárcena, M.A., Siervo, F.J., 2000. Ocean-surface and wind dynamics in the Atlantic Ocean off Northwest Africa during the last 140 000 years. *Palaeogeogr. Palaeoclimatol. Palaeoecol.* 161, 459–478. [https://doi.org/10.1016/S0031-0182\(00\)00099-7](https://doi.org/10.1016/S0031-0182(00)00099-7).
- Frigola, J., Moreno, A., Cacho, I., Canals, M., Siervo, F.J., Flores, J.A., Grimalt, J.O., 2008. Evidence of abrupt changes in Western Mediterranean Deep Water circulation during the last 50 kyr: a high-resolution marine record from the Balearic Sea. *Quat. Int.* 181, 88–104. <https://doi.org/10.1016/j.quaint.2007.06.016>.
- Gegen, R., Bordoni, S., Battisti, D.S., Hui, K., 2020. Monsoons, ITCZs, and the Concept of the Global Monsoon. *Rev. Geophys.* 58, e2020RG000700 <https://doi.org/10.1029/2020RG000700>.
- Girola, A., Capotondi, L., Ciaranfi, N., Di Leo, P., Lirer, F., Maiorano, P., Marino, M., Pelosi, N., Pulice, I., 2013. Paleoenvironmental changes at the lower Pleistocene Montalbano Jonico section (southern Italy): global versus regional signals. *Palaeogeogr. Palaeoclimatol. Palaeoecol.* 371, 62–79. <https://doi.org/10.1016/j.palaeo.2012.12.017>.
- Giunta, S., Negri, A., Morigi, C., Capotondi, L., Combourieu-Nebout, N., Emeis, K.C., Sangiorgi, F., Vigliotti, L., 2003. Coccolithophorid ecostratigraphy and multi-proxy paleoceanographic reconstruction in the Southern Adriatic Sea during the last deglacial time (Core AD91-17). *Palaeogeogr. Palaeoclimatol. Palaeoecol.* 190, 39–59. [https://doi.org/10.1016/S0031-0182\(02\)00598-9](https://doi.org/10.1016/S0031-0182(02)00598-9).
- Grant, K.M., Rohling, E.J., Bar-Matthews, M., Ayalon, A., Medina-Elizalde, M., Ramsey, C.B., Satow, C., Roberts, A.P., 2012. Rapid coupling between ice volume and polar temperature over the past 50,000 years. *Nature* 491, 744–747. <https://doi.org/10.1038/nature11593>.
- Grant, K.M., Grimm, R., Mikolajewicz, U., Marino, G., Ziegler, M., Rohling, E.J., 2016. The timing of Mediterranean sapropel deposition relative to insolation, sea-level and African monsoon changes. *Quat. Sci. Rev.* 140, 125–141. <https://doi.org/10.1016/j.quascirev.2016.03.026>.
- Grant, K.M., Rohling, E.J., Westerhold, T., Zabel, M., Heslop, D., Konijnendijk, T., Lourens, L., 2017. A 3 million year index for North African humidity/aridity and the implication of potential pan-African Humid periods. *Quat. Sci. Rev.* 171, 100–118. <https://doi.org/10.1016/j.quascirev.2017.07.005>.
- Grelaud, M., Marino, G., Ziveri, P., Rohling, E.J., 2012. Abrupt shoaling of the nutricline in response to massive freshwater flooding at the onset of the last interglacial sapropel event. *Paleoceanography* 27. <https://doi.org/10.1029/2012PA002288>.
- Guo, Z., Zhou, X., Wu, H., 2012. Glacial-interglacial water cycle, global monsoon and atmospheric methane changes. *Clim. Dyn.* 39, 1073–1092. <https://doi.org/10.1007/s00382-011-1147-5>.
- Hernández-Almeida, I., Ausín, B., Saavedra-Pellitero, M., Baumann, K.-H., Stoll, H.M., 2019. Quantitative reconstruction of primary productivity in low latitudes during the last glacial maximum and the mid-to-late Holocene from a global Florisphaera profunda calibration dataset. *Quat. Sci. Rev.* 205, 166–181. <https://doi.org/10.1016/j.quascirev.2018.12.016>.
- Hodell, D., Crowhurst, S., Skinner, L., Tzedakis, P.C., Margari, V., Channell, J.E.T., Kamenov, G., MacLachlan, S., Rothwell, G., 2013. Response of Iberian margin sediments to orbital and suborbital forcing over the past 420 ka. *Paleoceanography* 28, 185–199. <https://doi.org/10.1029/palo.20017>.
- Hodell, D., Lourens, L., Crowhurst, S., Konijnendijk, T., Tjallingii, R., Jiménez-Espejo, F., Skinner, L., Tzedakis, P.C., Abrantes, F., Acton, G.D., Alvarez Zarikian, C.A., Bahr, A., Balestra, B., Barranco, E.L., Carrara, G., Ducassou, E., Flood, R.D., Flores, J.-A., Furota, S., Grimalt, J., Grunert, P., Hernández-Molina, J., Kim, J.K., Krissek, L.A., Kuroda, J., Li, B., Lofli, J., Margari, V., Martrat, B., Miller, M.D., Nanayama, F., Nishida, N., Richter, C., Rodrigues, T., Rodríguez-Tovar, F.J., Roque, A.C.F., Sanchez Góñi, M.F., Sierra Sánchez, F.J., Singh, A.D., Sloss, C.R., Stow, D.A.V., Takashimizu, Y., Tzanova, A., Voelker, A., Xuan, C., Williams, T., 2015. A reference time scale for Site U1385 (Shackleton Site) on the SW Iberian Margin. *Glob. Planet. Chang.* 133, 49–64. <https://doi.org/10.1016/j.gloplacha.2015.07.002>.
- Incarbone, A., Di Stefano, E., 2019. Calcareous nannofossil palaeoenvironmental reconstruction and preservation in sapropel S1 at the Eratosthenes Seamount (Eastern Mediterranean). *Deep Sea Res Part II Top. Stud. Oceanogr.* 164, 206–215. <https://doi.org/10.1016/j.dsrrb.2018.10.004>.
- Incarbone, A., Di Stefano, E., Parti, B., Pelosi, N., Bonomo, S., Mazzola, S., Sprovieri, R., Tranchida, G., Zgozi, S., Bonanno, A., 2008. Holocene millennial-scale productivity variations in the Sicily Channel (Mediterranean Sea). *Paleoceanography* 23, 1–18. <https://doi.org/10.1029/2007PA001581>.
- Incarbone, A., Martrat, B., Di Stefano, E., Grimalt, J.O., Pelosi, N., Patti, B., Tranchida, G., 2010a. Primary productivity variability on the Atlantic Iberian margin over the last 70,000 years: evidence from coccolithophores and fossil organic compounds. *Paleoceanography* 25, 1–15. <https://doi.org/10.1029/2008PA001709>.
- Incarbone, A., Ziveri, P., Di Stefano, E., Lirer, F., Mortyn, G., Patti, B., Pelosi, N., Sprovieri, M., Tranchida, G., Vallefuoco, M., Albertazzi, S., Bellucci, L.G., Bonanno, A., Bonomo, S., Censi, P., Ferraro, L., Giuliani, S., Mazzola, S., Sprovieri, R., 2010b. The impact of the little ice age on coccolithophores in the Central Mediterranean Sea. *Clim. Past* 6, 795–805. <https://doi.org/10.5194/cp-6-795-2010>.
- Incarbone, A., Ziveri, P., Sabatino, N., Manta, D.S., Sprovieri, M., 2011. Conflicting coccolithophore and geochemical evidence for productivity levels in the Eastern Mediterranean sapropel S1. *Mar. Micropaleontol.* 81, 131–143. <https://doi.org/10.1016/j.marmicro.2011.09.003>.
- Incarbone, A., Sprovieri, M., Di Stefano, A., Di Stefano, E., Salvagio Manta, D., Pelosi, N., Ribera d'Alcalà, M., Sprovieri, R., Ziveri, P., 2013. Productivity modes in the mediterranean sea during dansgaard-oeschger (20,000–70,000yr ago) oscillations. *Palaeogeogr. Palaeoclimatol. Palaeoecol.* 392 <https://doi.org/10.1016/j.palaeo.2013.09.023>.
- Incarbone, A., Abu-Zied, R.H., Rohling, E.J., Ziveri, P., 2019. Reventilation episodes during the Sapropel S1 deposition in the Eastern Mediterranean based on holococcolith preservation. *Paleoceanogr. Paleoclimatol.* 34, 1597–1609. <https://doi.org/10.1029/2019PA003626>.
- Jordan, R.W., Cros, L., Young, J.R., 2004. A revised classification scheme for living haptophytes. *Micropaleontology* 50, 55–79. <https://doi.org/10.2113/50.Suppl.155>.
- Josey, S.A., Somot, S., Tsimplis, M., 2011. Impacts of atmospheric modes of variability on Mediterranean Sea surface heat exchange. *J. Geophys. Res. Ocean.* 116, 1–15. <https://doi.org/10.1029/2010JC006685>.
- Kemp, A.E.S., Pearce, R.B., Koizumi, I., Pike, J., Rance, S.J., 1999. The role of mat-forming diatoms in the formation of Mediterranean sapropels. *Nature* 398, 57.
- Kleijne, A., 1991. Holococcolithophorids from the Indian-Ocean, Red-Sea, Mediterranean-Sea and North-Atlantic Ocean. *Mar. Micropaleontol.* 17, 1–76. [https://doi.org/10.1016/0377-8398\(91\)90023-Y](https://doi.org/10.1016/0377-8398(91)90023-Y).
- Klein, P., Coste, B., 1984. Effects of wind-stress variability on nutrient transport into the mixed layer. *Deep Sea Res. Part A. Oceanogr. Res. Pap.* 31, 21–37. [https://doi.org/10.1016/0198-0149\(84\)90070-0](https://doi.org/10.1016/0198-0149(84)90070-0).
- Knappertsbusch, M., 1993. Geographic distribution of living and Holocene coccolithophores in the Mediterranean Sea. *Mar. Micropaleontol.* [https://doi.org/10.1016/0377-8398\(93\)90016-Q](https://doi.org/10.1016/0377-8398(93)90016-Q).
- Konijnendijk, T.Y.M., Ziegler, M., Lourens, L., 2014. Chronological constraints on Pleistocene sapropel depositions from high-resolution geochemical records of ODP Sites 967 and 968. *Newsl. Stratigr.* <https://doi.org/10.1127/0078-0421/2014/0047>.
- Konijnendijk, T.Y.M., Ziegler, M., Lourens, L.J., 2015. On the timing and forcing mechanisms of late Pleistocene glacial terminations: insights from a new high-resolution benthic stable oxygen isotope record of the eastern Mediterranean. *Quat. Sci. Rev.* 129, 308–320. <https://doi.org/10.1016/j.quascirev.2015.10.005>.
- Krebs, U., Timmermann, A., 2007. Tropical air-sea interactions accelerate the recovery of the atlantic meridional overturning circulation after a major shutdown. *J. Clim.* 20, 4940–4956. <https://doi.org/10.1175/JCLI4296.1>.

- Krom, M.D., Kress, N., Brenner, S., Gordon, L.I., 1991. Phosphorus limitation of primary productivity in the Eastern Mediterranean Sea. *Limnol. Oceanogr.* 36, 424–432.
- Krom, M.D., Emeis, K.C., Van Cappellen, P., 2010. Why is the Eastern Mediterranean phosphorus limited? *Prog. Oceanogr.* 85, 236–244. <https://doi.org/10.1016/j.pocean.2010.03.003>.
- Landaas, A., Dreyfus, G., Capron, E., Masson-Delmotte, V., Sanchez-Goñi, M.F., Desprat, S., Hoffmann, G., Jouzel, J., Leuenberger, M., Johnsen, S., 2010. What drives the millennial and orbital variations of $\delta^{18}\text{O}$? *Quat. Sci. Rev.* 29, 235–246. <https://doi.org/10.1016/j.quascirev.2009.07.005>.
- Larrasoña, J.C., Roberts, A.P., Rohling, E.J., Winklhofer, M., Wehausen, R., 2003. Three million years of monsoon variability over the northern Sahara. *Clim. Dyn.* 21, 689–698. <https://doi.org/10.1007/s00382-003-0355-z>.
- Laskar, J., Robutel, P., Joutel, F., Gastineau, M., Correia, A.C.M., Levrard, B., 2004. Astrophysics a long-term numerical solution for the insolation. *Astronomy* 285, 261–285. <https://doi.org/10.1051/0004-6361>.
- Lionello, P., 2012. The Climate of the Mediterranean Region: From the Past to the Future, 1st ed. Elsevier Inc. <https://doi.org/10.1016/B978-0-12-416042-2.00009-4>
- Lisiecki, L.E., Raymo, M.E., 2005. A Pliocene-Pleistocene stack of 57 globally distributed benthic 180 records. *Paleoceanography* 20, 1–17. <https://doi.org/10.1029/2004PA001071>.
- Loulouergue, L., Schilt, A., Spahni, R., Masson-Delmotte, V., Blunier, T., Lemieux, B., Barnola, J.-M., Raynaud, D., Stocker, T.F., Chappellaz, J., 2008. Orbital and millennial-scale features of atmospheric CH₄ over the past 800,000 years. *Nature* 453, 383–386. <https://doi.org/10.1038/nature06950>.
- Lourens, L.J., 2004. Revised tuning of Ocean Drilling Program Site 964 and KC01B (Mediterranean) and implications for the $\delta^{18}\text{O}$, tephra, calcareous nannofossil, and geomagnetic reversal chronologies of the past 1.1 Myr. *Paleoceanography* 19, 1–20. <https://doi.org/10.1029/2003PA000997>.
- Lourens, L.J., Wehausen, R., Brumsack, H.J., 2001. Geological constraints on tidal dissipation and dynamical ellipticity of the Earth over the past three million years. *Nature* 409, 1029.
- Maiorano, P., Tarantino, F., Marino, M., De Lange, G.J., 2013. Paleoenvironmental conditions at Core KC01B (Ionian Sea) through MIS 13–9: evidence from calcareous nannofossil assemblages. *Quat. Int.* 288, 97–111. <https://doi.org/10.1016/j.quaint.2011.12.007>.
- Malanotte-Rizzoli, P., Artale, V., Borzelli-Eusebi, G.L., Brenner, S., Crise, A., Gacic, M., Kress, N., Marullo, S., Ribera d'Alcalà, M., Sofianos, S., Tanhua, T., Theocaris, A., Alvarez, M., Ashkenazy, Y., Bergamasco, A., Cardin, V., Carniel, S., Civitarese, G., D'Ortenzio, F., Font, J., Garcia-Ladona, E., Garcia-Lafuente, J.M., Gogou, A., Gregoire, M., Hainbucher, D., Kontoyannis, H., Kovacevic, V., Kraskapoulou, E., Krookos, G., Incarbone, A., Mazzocchi, M.G., Orlík, M., Ozsoy, E., Pascual, A., Poulan, P.M., Roether, W., Rubino, A., Schroeder, K., Siokou-Frangou, J., Souvermezoglou, E., Sprovieri, M., Tintoré, J., Triantafyllou, G., 2014. Physical forcing and physical/biochemical variability of the Mediterranean Sea: a review of unresolved issues and directions for future research. *Ocean Sci.* 10, 281–322. <https://doi.org/10.5194/os-10-281-2014>.
- Malinverno, E., Triantaphyllou, M.V., Stavrakakis, S., Ziveri, P., Lykousis, V., 2009. Seasonal and spatial variability of coccolithophore export production at the South-Western margin of Crete (Eastern Mediterranean). *Mar. Micropaleontol.* 71, 131–147. <https://doi.org/10.1016/j.marmicro.2009.02.002>.
- Manabe, S., Stouffer, R.J., 1997. Coupled ocean-atmosphere model response to freshwater input: comparison to Younger Dryas Event. *Paleoceanography* 12, 321–336. <https://doi.org/10.1029/96PA03932>.
- Marino, G., Rohling, E.J., Rijpstra, W.I.C., Sangiorgi, F., Schouten, S., Sinnninghe Damsté, J.S., 2007. Aegean Sea as driver of hydrographic and ecological changes in the eastern Mediterranean. *Geology* 35, 675–678. <https://doi.org/10.1130/G23831A.1>.
- Marino, G., Rohling, E.J., Sangiorgi, F., Hayes, A., Casford, J.L., Lotter, A.F., Kucera, M., Brinkhuis, H., 2009. Early and middle Holocene in the Aegean Sea: interplay between high and low latitude climate variability. *Quat. Sci. Rev.* 28, 3246–3262. <https://doi.org/10.1016/j.quascirev.2009.08.011>.
- Marino, G., Rohling, E.J., Rodríguez-Sanz, L., Grant, K.M., Heslop, D., Roberts, A.P., Stanford, J.D., Yu, J., 2015. Bipolar seesaw control on last interglacial sea level. *Nature* 522, 197–201. <https://doi.org/10.1038/nature14499>.
- Marino, M., Maiorano, P., Lirer, F., 2008. Changes in calcareous nannofossil assemblages during the Mid-Pleistocene Revolution. *Mar. Micropaleontol.* 69, 70–90. <https://doi.org/10.1016/j.marmicro.2007.11.010>.
- Martrat, B., Grimalt, J.O., Shackleton, N.J., de Abreu, L., Hutterli, M.A., Stocker, T.F., 2007. Four climate cycles of recurring deep and surface water destabilizations on the Iberian margin. *Science* 317, 502–507. <https://doi.org/10.1126/science.1139994>.
- Martrat, B., Jimenez-Amat, P., Zahn, R., Grimalt, J.O., 2014. Similarities and dissimilarities between the last two deglaciations and interglaciations in the North Atlantic region. *Quat. Sci. Rev.* 99, 122–134. <https://doi.org/10.1016/j.quascirev.2014.06.016>.
- McIntyre, A., Molino, B., 1996. Forcing of atlantic equatorial and subpolar millennial cycles by precession. *Science*. <https://doi.org/10.1126/science.274.5294.1867>.
- McManus, J.F., Oppo, D.W., Cullen, J.L., 1999. A 0.5-million-year record of millennial-scale climate variability in the North Atlantic. *Science* 283.
- McManus, J.F., Francois, R., Gherardi, J.-M., Keigwin, L.D., Brown-Leger, S., 2004. Collapse and rapid resumption of Atlantic meridional circulation linked to deglacial climate changes. *Nature* 428, 834–837. <https://doi.org/10.1038/nature02494>.
- van der Meer, M.T.J., Baas, M., Rijpstra, W.I.C., Marino, G., Rohling, E.J., Sinnninghe Damsté, J.S., Schouten, S., 2007. Hydrogen isotopic compositions of long-chain alkenones record freshwater flooding of the Eastern Mediterranean at the onset of sapropel deposition. *Earth Planet. Sci. Lett.* 262, 594–600. <https://doi.org/10.1016/j.epsl.2007.08.014>.
- Meier, K.J.S., Zonneveld, K.A.F., Kasten, S., Willems, H., 2004. Different nutrient sources forcing increased productivity during eastern Mediterranean S1 sapropel formation as reflected by calcareous dinoflagellate cysts. *Paleoceanography* 19, 1–12. <https://doi.org/10.1029/2003PA000895>.
- Millot, C., 1999. Circulation in the Western Mediterranean Sea. *J. Mar. Syst.* 20, 423–442. [https://doi.org/10.1016/S0924-7963\(98\)00078-5](https://doi.org/10.1016/S0924-7963(98)00078-5).
- Molfino, B., McIntyre, A., 1990a. Precessional forcing of nutricline dynamics in the equatorial Atlantic. *Science* 249, 766–769. <https://doi.org/10.1126/science.249.4970.766>.
- Molfino, B., McIntyre, A., 1990b. Nutricline variation in the equatorial Atlantic coincident with the Younger Dryas. *Paleoceanography*. <https://doi.org/10.1029/PA0051006p00997>.
- Möller, L., Sowers, T., Bock, M., Spahni, R., Behrens, M., Schmitt, J., Miller, H., Fischer, H., 2013. Independent variations of CH₄ emissions and isotopic composition over the past 160,000 years. *Nat. Geosci.* 6, 885–890. <https://doi.org/10.1038/ngeo1922>.
- Moulin, C., Lambert, C., Dulac, F., et al., 1997. Control of atmospheric export of dust from North Africa by the North Atlantic Oscillation. *Nature* 387, 691–694. <https://doi.org/10.1038/42679>.
- Myers, P.G., Haines, K., Rohling, E.J., 1998. Modeling the paleocirculation of the Mediterranean: the last glacial maximum and the Holocene with emphasis on the formation of sapropel S1. *Paleoceanography* 13, 586–606.
- Negri, A., Capotondi, L., Keller, J., 1999. Calcareous nannofossils, planktonic foraminifera and oxygen isotopes in the late Quaternary sapropels of the Ionian Sea. *Mar. Geol.* 157, 89–103. [https://doi.org/10.1016/S0025-3227\(98\)00135-2](https://doi.org/10.1016/S0025-3227(98)00135-2).
- Nicholson, S.L., Pike, A.W.G., Hosfield, R., Roberts, N., Sahy, D., Woodhead, J., Cheng, H., Edwards, R.L., Affolter, S., Leuenberger, M., Burns, S.J., Matter, A., Fleitmann, D., 2020. Pluvial periods in Southern Arabia over the last 1.1 million years. *Quat. Sci. Rev.* 229, 106112. <https://doi.org/10.1016/j.quascirev.2019.106112>.
- Oppo, D.W., Keigwin, L.D., McManus, J.F., 2001. Persistent suborbital climate variability in marine isotope stage 5 and Termination II. *Paleoceanography* 16, 280–292.
- Oppo, D.W., McManus, J.F., Cullen, J.L., 2006. Evolution and demise of the Last Interglacial warmth in the subpolar North Atlantic. *Quat. Sci. Rev.* 25, 3268–3277. <https://doi.org/10.1016/j.quascirev.2006.07.006>.
- Osborne, A.H., Vance, D., Rohling, E.J., Barton, N., Rogerson, M., Fello, N., 2008. A humid corridor across the Sahara for the migration of early modern humans out of Africa 120,000 years ago. *Proc. Natl. Acad. Sci. U. S. A.* 105, 16444–16447. <https://doi.org/10.1073/pnas.0804472105>.
- Ovchinnikov, I.M., 1984. The formation of Intermediate Water in the Mediterranean. *Oceanology* 24, 168–173.
- Oviedo, A., Ziveri, P., Álvarez, M., Tanhua, T., 2015. Is coccolithophore distribution in the Mediterranean Sea related to seawater carbonate chemistry? *Ocean Sci.* 11, 13–32. <https://doi.org/10.5194/os-11-13-2015>.
- Petrenko, V.V., Smith, A.M., Brook, E.J., Lowe, D., Riedel, K., Brailescu, G., Hua, Q., Schaefer, H., Reeh, N., Weiss, R.F., Etheridge, D., Severinghaus, J.P., 2009. Measurements in greenland ice: investigating last glacial termination CH₄ sources. *Science* (80-) 324, 506–508. <https://doi.org/10.1126/science.1168909>.
- Pinardi, N., Masetti, E., 2000. Variability of the large scale general circulation of the Mediterranean Sea from observations and modelling: a review. *Palaeogeogr. Palaeoclimatol. Palaeoecol.* 158, 153–174. [https://doi.org/10.1016/S0031-0182\(00\)00048-1](https://doi.org/10.1016/S0031-0182(00)00048-1).
- POE group, 1992. General-Circulation of the Eastern Mediterranean. *Earth-Science Rev.* 32, 285–309.
- Porter, S.C., Zhisheng, A., 1995. Correlation between climate events in the North Atlantic and China during the last glaciation. *Nature* 375, 305–308. <https://doi.org/10.1038/375305a0>.
- Principato, M.S., Crudeli, D., Ziveri, P., Slomp, C.P., Corselli, C., Erba, E., de Lange, G.J., 2006. Phyto- and zooplankton paleofluxes during the deposition of sapropel S1 (eastern Mediterranean): Biogenic carbonate preservation and paleoecological implications. *Palaeogeogr. Palaeoclimatol. Palaeoecol.* 235, 8–27. <https://doi.org/10.1016/j.palaeo.2005.09.021>.
- Robinson, A.R., Golnaraghi, M., 1994. The physical and dynamical oceanography of the Mediterranean Sea. In: *Ocean Processes in Climate Dynamics: Global and Mediterranean Examples*, pp. 255–306. https://doi.org/10.1007/978-94-011-0870-6_12.
- Rodríguez-Sanz, L., Bernasconi, S.M., Marino, G., Heslop, D., Müller, I.A., Fernandez, A., Grant, K.M., Rohling, E.J., 2017. Penultimate deglacial warming across the Mediterranean Sea revealed by clumped isotopes in foraminifera. *Sci. Rep.* 7, 16572. <https://doi.org/10.1038/s41598-017-16528-6>.
- Rogalla, U., Andruleit, H., 2005. Precessional forcing of coccolithophore assemblages in the northern Arabian Sea: implications for monsoonal dynamics during the last 200,000 years. *Mar. Geol.* 217, 31–48. <https://doi.org/10.1016/j.margeo.2005.02.028>.
- Rohling, E.J., 1991a. Shoaling of the Eastern Mediterranean Pycnocline due to reduction of excess evaporation: implications for sapropel formation. *Paleoceanography* 6, 747–753. <https://doi.org/10.1029/91PA02455>.
- Rohling, E.J., 1991b. A simple two-layered model for shoaling of the eastern Mediterranean pycnocline due to Glacio-Eustatic sea level lowering. *Paleoceanography* 6, 537–541. <https://doi.org/10.1029/91PA01328>.
- Rohling, E.J., Gieskes, W.W., 1989. Late Quaternary changes in Mediterranean intermediate water density and formation rate. *Paleoceanography* 4, 531–545.
- Rohling, E.J., Cane, T.R., Cooke, S., Sprovieri, M., Bouloubassi, I., Emeis, K.C., Schiebel, R., Kroon, D., Jorissen, F.J., Lorre, A., Kemp, A.E.S., 2002a. African monsoon variability during the previous interglacial maximum. *Earth Planet. Sci. Lett.* 202, 61–75. [https://doi.org/10.1016/S0012-821X\(02\)00775-6](https://doi.org/10.1016/S0012-821X(02)00775-6).

- Rohling, E.J., Mayewski, P., Abu-Zied, R., Casford, J., Hayes, A., 2002b. Holocene atmosphere-ocean interactions: records from Greenland and the Aegean Sea. *Clim. Dyn.* 18, 587–594. <https://doi.org/10.1007/s00382-001-0194-8>.
- Rohling, E.J., Sprovieri, M., Cane, T., Casford, J.S.L., Cooke, S., Bouloubassi, I., Emeis, K.C., Schiebel, R., Rogerson, M., Hayes, A., Jorissen, F.J., Kroon, D., 2004. Reconstructing past planktic foraminiferal habitats using stable isotope data: a case history for Mediterranean sapropel S5. *Mar. Micropaleontol.* 50, 89–123. [https://doi.org/10.1016/S0377-8398\(03\)00068-9](https://doi.org/10.1016/S0377-8398(03)00068-9).
- Rohling, E.J., Hopmans, E.C., Damsté, J.S.S., 2006. Water column dynamics during the last interglacial anoxic event in the Mediterranean (sapropel S5). *Paleoceanography* 21, 1–8. <https://doi.org/10.1029/2005PA001237>.
- Rohling, E.J., Foster, G.L., Grant, K.M., Marino, G., Roberts, A.P., Tamisiea, M.E., Williams, F., 2014. Sea-level and deep-sea-temperature variability over the past 5.3 million years. *Nature* 508, 477–482. <https://doi.org/10.1038/nature13230>.
- Rohling, E.J., Marino, G., Grant, K.M., 2015. Mediterranean climate and oceanography, and the periodic development of anoxic events (sapropels). *Earth-Science Rev.* 143, 62–97. <https://doi.org/10.1016/j.earscirev.2015.01.008>.
- Rohling, E.J., Marino, G., Grant, K.M., Mayewski, P.A., Weninger, B., 2019. A model for archaeologically relevant Holocene climate impacts in the Aegean-Levantine region (easternmost Mediterranean). *Quat. Sci. Rev.* 208, 38–53. <https://doi.org/10.1016/j.quascirev.2019.02.009>.
- Rohling, Eelco J., Kemp, A.E.S., Cooke, S., Pearce, R.B., 2002. High-resolution stratigraphic framework for Mediterranean sapropel S5: defining temporal relationships between records of Eemian climate variability. *Palaeogeogr. Palaeoclimatol. Palaeoecol.* 183, 87–101. [https://doi.org/10.1016/S0031-0182\(01\)00461-8](https://doi.org/10.1016/S0031-0182(01)00461-8).
- Rossignol-Strick, M., Nesteroff, W., Olive, P., Vergnaud-Grazzini, C., 1982. After the deluge: Mediterranean stagnation and sapropel formation. *Nature* 295, 105.
- Roth, P.H., Coulbourn, W.T., 1982. Flora and solution patterns of coccoliths in surface sediments of the North Pacific. *Mar. Micropaleontol.* 7, 1–52. [https://doi.org/10.1016/0377-8398\(82\)90014-7](https://doi.org/10.1016/0377-8398(82)90014-7).
- Sakamoto, T., Janecek, T., Emeis, K., 1998. Continuous Sedimentary Sequences From the Eastern Mediterranean Sea: Composite Depth Sections 1–160, pp. 37–59.
- Satow, C., Tomlinson, E.L., Grant, K.M., Albert, P.G., Smith, V.C., Manning, C.J., Ottolini, L., Wulf, S., Rohling, E.J., Lowe, J.J., Blockley, S.P.E., Menzies, M.A., 2015. A new contribution to the Late Quaternary tephrostratigraphy of the Mediterranean: Aegean Sea core LC21. *Quat. Sci. Rev.* 117, 96–112. <https://doi.org/10.1016/j.quascirev.2015.04.005>.
- Schrag, D.P., Adkins, J.F., McIntyre, K., Alexander, J.L., Hodell, D.A., Charles, C.D., McManus, J.F., 2002. The oxygen isotopic composition of seawater during the last Glacial Maximum. *Quat. Sci. Rev.* 21, 331–342.
- Schulz, H., Rad, U., Erlenkeuser, H., 1998. Correlations between Arabian Sea and Greenland climate oscillations of the past 110,000 years. *Nature* 393, 54–57.
- Sierro, F.J., Hodell, D.A., Curtis, J.H., Flores, J.A., Reguera, I., Colmenero-Hidalgo, E., Bárcena, M.A., Grimalt, J.O., Cacho, I., Frigola, J., Canals, M., 2005. Impact of iceberg melting on Mediterranean thermohaline circulation during Heinrich events. *Paleoceanography* 20, 1–13. <https://doi.org/10.1029/2004PA001051>.
- Sierro, F.J., Hodell, D.A., Andersen, N., Azibeiro, L.A., Jimenez-Espejo, F.J., Bahr, A., Flores, J.A., Ausin, B., Rogerson, M., Lozano-Luz, R., Lebreiro, S.M., Hernandez-Molina, F.J., 2020. Mediterranean Overflow over the last 250 kyr: Freshwater Forcing from the Tropics to the Ice Sheets. *Paleoceanogr. Paleoclimatol.* 35, e2020PA003931 <https://doi.org/10.1029/2020PA003931>.
- Sirocko, F., Sarnthein, M., Erlenkeuser, H., Lange, H., Arnold, M., Duplessy, J.C., 1993. Century-scale events in monsoonal climate over the past 24,000 years. *Nature* 364, 322–324. <https://doi.org/10.1038/364322a0>.
- Skampa, E., Triantaphyllou, M.V., Dimiza, M.D., Gogou, A., Malinverno, E., Stavrakakis, S., Panagiotopoulos, I.P., Parinos, C., Baumann, K.-H., 2019. Coupling plankton - sediment trap - surface sediment coccolithophore regime in the North Aegean Sea (NE Mediterranean). *Mar. Micropaleontol.* 152, 101729.
- Spratt, R.M., Lisicki, L.E., 2016. A Late Pleistocene sea level stack. *Clim. Past* 12, 1079–1092. <https://doi.org/10.5194/cp-12-1079-2016>.
- Sprovieri, M., Di Stefano, E., Incarbone, A., Salvagio Manta, D., Pelosi, N., Ribera d'Alcalà, M., Sprovieri, R., 2012. Centennial- to millennial-scale climate oscillations in the Central-Eastern Mediterranean Sea between 20,000 and 70,000 years ago: evidence from a high-resolution geochemical and micropaleontological record. *Quat. Sci. Rev.* 46, 126–135. <https://doi.org/10.1016/j.quascirev.2012.05.005>.
- Stockhecke, M., Timmermann, A., Kipfer, R., Haug, G.H., Kwiecien, O., Friedrich, T., Menviel, L., Litt, T., Pickarski, N., Anselmetti, F.S., 2016. Millennial to orbital-scale variations of drought intensity in the Eastern Mediterranean. *Quat. Sci. Rev.* 133, 77–95. <https://doi.org/10.1016/j.quascirev.2015.12.016>.
- Thirumalai, K., Quinn, T.M., Marino, G., 2016. Constraining past seawater $\delta^{18}\text{O}$ and temperature records developed from foraminiferal geochemistry. *Paleoceanography* 31, 1409–1422. <https://doi.org/10.1002/2016PA002970>.
- Tierney, J.E., Russell, J.M., Huang, Y., Damsté, J.S.S., Hopmans, E.C., Cohen, A.S., 2008. Northern Hemisphere controls on Tropical Southeast African climate during the past 60,000 years. *Science* (80-.) 322, 252–255. <https://doi.org/10.1126/science.1160485>.
- Tjallingii, R., Claussen, M., Stuut, J.B.W., Fohlmeister, J., Jahn, A., Bickert, T., Lamy, F., Röhl, U., 2008. Coherent high- and low-latitude control of the northwest African hydrological balance. *Nat. Geosci.* 1, 670–675. <https://doi.org/10.1038/ngeo289>.
- Toucanne, S., Jouet, G., Ducassou, E., Bassetti, M.A., Dennielou, B., Angue Minto'o, C.M., Lahmi, M., Touyet, N., Charlier, K., Lercolais, G., Mulder, T., 2012. A 130,000-year record of Levantine Intermediate Water flow variability in the Corsica Trough, western Mediterranean Sea. *Quat. Sci. Rev.* 33, 55–73. <https://doi.org/10.1016/j.quascirev.2011.11.020>.
- Triantaphyllou, M.V., Ziveri, P., Tselepides, A., 2004. Coccolithophore export production and response to seasonal surface water variability in the oligotrophic Cretan Sea (NE Mediterranean). *Micropaleontology* 50, 127–144.
- Triantaphyllou, M.V., Antonarakou, A., Kouli, K., Dimiza, M.D., Kontakiotis, G., Papanikolaou, M.D., Ziveri, P., Mortyn, P.G., Lianou, V., Lykousis, V., Dermitzakis, M.D., 2009a. Late Glacial-Holocene ecostratigraphy of the South-Eastern Aegean Sea, based on plankton and pollen assemblages. *Geo-Marine Lett.* 29, 249–267. <https://doi.org/10.1007/s00367-009-0139-5>.
- Triantaphyllou, M.V., Ziveri, P., Gogou, A., Marino, G., Lykousis, V., Bouloubassi, I., Emeis, K.C., Kouli, K., Dimiza, M.D., Rosell-Melé, A., Papanikolaou, M., Katsouras, G., Nunez, N., 2009b. Late Glacial-Holocene climate variability at the south-eastern margin of the Aegean Sea. *Mar. Geol.* 266, 182–197. <https://doi.org/10.1016/j.margeo.2009.08.005>.
- Triantaphyllou, M.V., Antonarakou, A., Dimiza, M.D., Anagnostou, C., 2010. Calcareous nannofossil and planktonic foraminiferal distributional patterns during deposition of sapropels S6, S5 and S1 in the Libyan Sea (Eastern Mediterranean). *Geo-Marine Lett.* 30, 1–13. <https://doi.org/10.1007/s00367-009-0145-7>.
- Tzedakis, P.C., Drysdale, R.N., Margari, V., Skinner, L.C., Menviel, L., Rhodes, R.H., Taschetto, A.S., Hodell, D.A., Crowhurst, S.J., Hellstrom, J.C., Fallick, A.E., Grimalt, J.O., McManus, J.F., Martrat, B., Mokeddem, Z., Parrenin, F., Regattieri, E., Roe, K., Zanchetta, G., 2018. Enhanced climate instability in the North Atlantic and southern Europe during the last Interglacial. *Nat. Commun.* 9, 4235. <https://doi.org/10.1038/s41467-018-06683-3>.
- Velaoras, D., Papadopoulos, V.P., Kontoyiannis, H., Papageorgiou, D.K., Pavlidou, A., 2017. The Response of the Aegean Sea (Eastern Mediterranean) to the Extreme 2016–2017 Winter. *Geophys. Res. Lett.* 44, 9416–9423. <https://doi.org/10.1002/2017GL074761>.
- Vellinga, M., Wood, R.A., 2002. Global climatic impacts of a collapse of the atlantic thermohaline circulation. *Clim. Chang.* 54, 251–267. <https://doi.org/10.1023/A:1016168827653>.
- Veres, D., Bazin, L., Landais, A., Toyé Mahamadou Kele, H., Lemieux-Dudon, B., Parrenin, F., Martinerie, P., Blayo, E., Blunier, T., Capron, E., Chappellaz, J., Rasmussen, S.O., Severi, M., Svensson, A., Vinther, B., Wolff, E.W., 2013. The Antarctic ice core chronology (AICC2012): an optimized multi-parameter and multi-site dating approach for the last 120 thousand years. *Clim. Past* 9, 1733–1748. <https://doi.org/10.5194/cp-9-1733-2013>.
- Wehausen, R., Brumsack, H., 2000. Chemical cycles in Pliocene sapropel-bearing and sapropel-barren eastern Mediterranean sediments. *Palaeogeogr. Palaeoclimatol. Palaeoecol.* 158, 325–352.
- Young, J.R., 1994. Functions of coccoliths. In: Winter, A., Siesser, W.G. (Eds.), *Coccolithophores*. Cambridge Univ. Press, Cambridge, pp. 63–82.
- Young, J.R., Geisen, M., Cros, L., Kleijne, A., Sprengel, C., Probert, I., Østergaard, J., 2003. A guide to extant coccolithophore taxonomy. *J. Nannoplankt. Res.* 125.
- Zabel, M., Bickert, T., Dittert, L., Haese, R.R., 1999. Significance of the sedimentary Al:Ti ratio as an indicator for variations in the circulation patterns of the equatorial North Atlantic. *Paleoceanography* 14 (6), 789–799. <https://doi.org/10.1029/1999PA900027>.
- Zhang, R., Delworth, T.L., 2006. Impact of Atlantic multidecadal oscillations on India/Sahel rainfall and Atlantic hurricanes. *Geophys. Res. Lett.* 33 <https://doi.org/10.1029/2006GL026267>.
- Ziegler, M., Lourens, L.J., Tuenter, E., Hilgen, F., Reichart, G.-J., Weber, N., 2010. Precession phasing offset between Indian summer monsoon and Arabian Sea productivity linked to changes in Atlantic overturning circulation. *Paleoceanography* 25, 1–16. <https://doi.org/10.1029/2009PA001884>.
- Ziveri, P., Thunell, R.C., 2000. Coccolithophore export production in Guaymas Basin, Gulf of California: response to climate forcing. *Deep-Sea Res. II* 47, 2073–2100. [https://doi.org/10.1016/S0967-0645\(00\)00017-5](https://doi.org/10.1016/S0967-0645(00)00017-5).
- Ziveri, P., Broerse, A.T.C., van Hinte, J.E., Westbroek, P., Honjo, S., 2000. The fate of coccoliths at 48°N 21°W, Northeastern Atlantic. *Deep Sea Res Part II Top. Stud. Oceanogr.* 47, 1853–1875. [https://doi.org/10.1016/S0967-0645\(00\)00009-6](https://doi.org/10.1016/S0967-0645(00)00009-6).